

A.I.F.A. - ITALIAN ASSOCIATION FOR FATIGUE IN AERONAUTICS
DEPARTMENT OF CIVIL AND INDUSTRIAL ENGINEERING - UNIVERSITY OF PISA

Review of aeronautical fatigue investigations
carried out in Italy
during the period April 2011 - March 2013

by
L. Lazzeri
Department of Civil and Industrial Engineering
University of Pisa - Italy

This document summarizes the main research activities carried out in Italy about aeronautical fatigue in the period April 2011 – March 2013. The main topics covered are: load analysis, fatigue and fracture mechanics of metallic structures, fatigue and damage tolerance behaviour of composites, full scale testing.

33rd ICAF Conference, Jerusalem, Israel, 3-4 June 2013

CONTENTS

	Page
1. INTRODUCTION	7/1
2. MEASUREMENT AND ANALYSIS OF OPERATIONAL LOADS	7/1
2.1 - Taxi spectra from semi-prepared runaways (Alenia Aermacchi)	7/1
2.2 - AM-X life monitoring (Alenia Aermacchi)	7/1
2.3 - Life monitoring of the TORNADO fleet (Alenia Aermacchi)	7/2
2.4 - EF Typhoon life monitoring (Alenia Aermacchi)	7/2
2.5 - Fibre optic sensors application for structural health monitoring (AgustaWestland)	7/2
2.6 - Health and Usage Monitoring System for AW101 helicopter (AgustaWestland)	7/3
2.7 - G222 program (Alenia Aermacchi)	7/3
3. METALS	7/4
3.1 - Fatigue behaviour of notched and unnotched materials	7/4
3.1.1 - Evaluation of mechanical milling solutions instead of chemical milling (Alenia Aermacchi)	7/4
3.1.2 - Fatigue behaviour of Inconel 718 coupons (Univ. Pisa)	7/4
3.1.3 - Developments of numerical simulation of the Laser Shock Peening process (Univ. Bologna)	7/4
3.2 - Crack propagation and fracture mechanics	7/6
3.2.1 - Damage Tolerance evaluation of flat panels stiffened by bonded pads (Univ. Pisa)	7/6
3.2.2 - Damage tolerance characterization of Mg cast alloys (AgustaWestland)	7/6
4. COMPOSITES AND FIBER METAL LAMINATES	7/7
4.1 - A novel cohesive zone modelling approach to evaluate Damage Tolerance of composite laminates (Milan Polytechnic)	7/7
4.2 - Interlaminar Fracture Mechanics characterization of composites (Univ. Pisa)	7/7
5. COMPONENT AND FULL-SCALE TESTING	7/7
5.1 - Development fatigue test of M-346 components (Alenia Aermacchi)	7/7
5.2 - M-346 Certification Full Scale and Component fatigue tests (Alenia Aermacchi)	7/8
6. AIRCRAFT FATIGUE SUBSTANTIATION	7/11
6.1 - Development of the Bombardier CSeries (Alenia Aermacchi)	7/11
6.2 - AW109 family (AgustaWestland)	7/11
6.3 - EH101 / AW101 helicopter family (AgustaWestland)	7/12
6.4 - AW189/ AW139 / AW169 helicopter family (AgustaWestland)	7/12
6.5 - AW139 helicopter LIPS demonstration (AgustaWestland)	7/12
6.6 - AW609 development (AgustaWestland)	7/13
6.7 - UAS Technology (Alenia Aermacchi)	7/13
7. REFERENCES	7/13
FIGURES AND TABLES	7/14

1. INTRODUCTION

This paper summarises aeronautical fatigue investigations which have been carried out in Italy during the period April 2011 to March 2013. The different contributions have been arranged according to the topics, which are loading analysis, fatigue and fracture mechanics of metallic materials, fatigue and damage tolerance behaviour of composites and full scale component testing. A list of references, related to the various items, is presented at the end of the document.

The review is based on the activities carried out within the various organisations belonging to A.I.F.A., the Italian Association for Fatigue in Aeronautics. The author gratefully acknowledges the fundamental contribution, which has made this review possible, given by several A.I.F.A. members, who are the representatives of Universities and Industries in A.I.F.A.

2. MEASUREMENT AND ANALYSIS OF OPERATIONAL LOADS

2.1 - Taxi spectra from semi-prepared runways (Alenia Aermacchi)

Within the framework of the Russian Certification of the ATR program, it has been required to compare and evaluate the differences between the original Design Taxi Spectra with respect to the in-service one.

Safe aircraft operations may be jeopardized when runways pavements are not smooth or even. Un-evenness may not only cause excessive accelerations and loads on aircraft tyres, landing gears and relevant back-up structure, but also discomfort for passengers and pilots, leading to degraded controllability during take-off and landing, tyre burst and structural damage of the aircraft.

The ATR Design Taxi Spectra (paved runway) has been compared to the Taxi Spectra measured on the main semi-prepared Russian runways; at the end of the comparison, the Fatigue Severity Factors (Damage on Semi-prepared /Damage on Paved) are provided for each analysed Russian runway. Fig. 1 shows the elevation profiles vs. length of a number of semi-prepared Russian runways, object of the evaluation.

The standard analysis approach has been the following:

- Determination of the Load Factor Spectra at aircraft CG by the Power Spectral Density analysis;
- Determination of cumulative frequency distribution for each segment;
- Stepping the above cumulative frequency distribution;
- Damage calculation using S-N curves and Miner's rule.

According to this procedure, it was possible to define a Severity Factor for each runway, as the ratio of the damage calculated in this way with respect to the damage of the design spectrum. A plot of the Cumulative Frequency Distribution of the vertical acceleration variations is shown in Fig. 2.

An alternative method to determine runway fatigue severity without fatigue damage calculation has been evaluated. The alternative analysis approach has been the following:

- Extract the runway profile;
- Determine the total cumulative dips and bumps of runway;
- Compare it with a reference basic value;
- Classify the runway in terms of equivalent fatigue damage.

This different approach has not been helpful, because it has been realized that the only bumps and dips distribution is not sufficient to quantify the effective runway taxi severity, and consequently the damage. This difficulty is due to the importance of dips and bumps relative positioning, distribution and severity; their effect is amplified by the aircraft speed. Moreover, the whole aircraft reacts to the disturbances keeping in mind also the previous load history.

2.2 - AM-X life monitoring (Alenia Aermacchi)

On AMX aircraft, fatigue monitoring is performed by means of classic mechanical g-meter readings and on the basis of provided information about configurations and mission profiles. Up to now, 187000 flight hours (corresponding to 182700 flights) have been monitored since the aircraft entered into service.

The Load Severity Index (L.S.I.), defined as the ratio between the In-Service Life Damage and the Design Life Usage, shows an average value (among the entire fleet) just above 1. Therefore fatigue life consumption is substantially in line with design assumptions. The L.S.I. trend as a function of time has arrested the raise shown in recent years and is now slightly decreasing, see Fig. 3; this figure is an update of a similar one present in the last National Review.

As an additional information, Fig. 4 shows the distribution of the L.S.I. index within the AM-X fleet: the usage severity is rather uniform.

2.3 - Life monitoring of the TORNADO fleet (Alenia Aermacchi)

Fatigue monitoring has been performed on I.A.F. Tornado, since its entry into service in 1980, by means of the own computer program that makes use of mechanical g-meter readings together with configuration/masses control. In total, 255300 flights hours (corresponding to 201000 flights) have been monitored so far. Among the 5 (4 + 1 dummy) monitored locations, the lower wing panel remains the most fatigue affected. However, the load severity index, even with a small increase, is definitely below 1. Fig. 5 shows the L.S.I. distribution for the strike and trainer aircraft, that is an update of similar data shown in the previous National Review.

Since the aircraft service life has been extended from 4000 up to 6000 Flight Hours, in order to assure that a correct fleet management is performed and any possible anomalous fatigue consumption is identified, the individual tracking will be maintained. Furthermore a new upgraded monitoring system is currently being developed.

2.4 - EF Typhoon life monitoring (Alenia Aermacchi)

Since 2003, 64 EF Typhoon aircrafts (52 single seat and 12 twin seat) have been delivered to the Italian Air Force. Since entry into service (2005), a total of 34000 Flight Hours (corresponding to 25000 Flights) have been flown, as for September 2012. The fleet leaders are now approaching 1000 FHs.

The Production Major Airframe Fatigue Test (PMAFT) is ongoing within BAEs facilities at Brough (UK). At the moment 12000 Flight Hours have been simulated (with design spectrum). Fin Buffet is also introduced by means of a dedicated arrangement making use of a dynamic stinger.

Alenia Aermacchi is engaged in an activity for the fleet fatigue and usage support by means of the Structural Health Monitoring system (SHM), including also the analysis of the SHM data. The SHM system provides:

- the **Fatigue Index calculation** for 10 structural significant location: this value indicates the fatigue life consumption;
- the **Auxiliary Data** relevant to flight data (g, roll rate, Mach, weight, altitude, etc): these data are not directly used for fatigue calculations, but can be used for specific analyses;
- the **Event Monitor** that points out any significant structural event compared to pertinent envelopes.

Among the Auxiliary data, g exceedences are counted by a computer based algorithm which simulates the mechanical g-meter behaviour. Hence it is possible to easily represent the in-flight registered g-spectrum and compare it to the design one. The In-service usage shows a spectrum shape similar to design assumptions, but definitely less severe. This trend is confirmed in Fatigue Indexes calculations, that are below design too (see Fig. 6).

2.5 - Fibre optic sensors application for structural health monitoring (AgustaWestland)

A research program has been started by AgustaWestland with the aim of demonstrating a new approach for the realization and test of an apparatus for FOBG (Fibre Optic Bragg Grating) sensors interrogation. The task is motivated by the need to identify a robust and reliable instrumentation for flight test campaign; for this purpose, AgustaWestland has instrumented a prototype to monitor periodically the sensors reliability and robustness.

The actions to develop are devoted to the identification of a new class of commercial devices and/or systems for the integration of a novel instrumentation which should be qualified for flight test campaign and, at the same time, must provide higher performances than conventional equipments.

Fibre Bragg gratings are the most popular fibre based sensors and have been chosen for this program as they are small, lightweight, easily installable onto/into host structures. Moreover, they have the following advantages:

- insensitive to electromagnetic fields;
- suffer no mechanical failure of sensor material (glass) under high vibration loads;
- reduced numbers of connection lines and hence less impact on test objectives of 10 million load cycles at $\pm 3.000 \mu\text{m/m}$ alternating strain.

An A109SP prototype helicopter rear fuselage, baggage compartment, was selected as the best candidate for the application and testing of the SHM technologies, mainly because of the following reasons:

- it is a typical aeronautical shell structure, consisting of a skin stiffened with frames and stringers;
- it is a part which is easy to access and available for visual or conventional inspection;
- there is a large number of riveted connections.

Fig. 7 shows a picture of the instrumented part. A measurement system for FBG sensors is composed essentially by:

- the FBG sensors themselves;
- the fibre optic cable for connection of the sensors with the interrogation unit;
- the interrogation unit itself, including signal conditioning, demodulation and data transmission;

- a computer for data storage and processing, connected with the interrogation unit through the Ethernet.

The sensing methods were developed within European Defense Agency sponsored project 'HECTOR', mentioned in the last National Review, in which the performance of different methodologies were evaluated in a laboratory environment. The critical step now is to validate the reliability and robustness in service and the probability of false information. For this reason, 'HECTOR' is followed by another EDA sponsored project named 'ASTIANAX' which started in February 2013.

Preliminary flight test data look very promising, with a clear identification of the different flight phases; the strain signal is quite clean, with a low noise level. Fig. 8 shows a record of the strain - time history collected.

2.6 - Health and Usage Monitoring System for AW139 helicopter (AgustaWestland)

In the previous review, information was given about activities carried out by AgustaWestland for the development of Enhanced Structural Usage Monitoring (ESUM) and Transmission Usage Monitoring (TUM) to improve the evaluation of fatigue loading spectra. These usage monitoring systems are installed on AW101 variants, AW139 and NH90.

In the period of the present review, efforts have been concentrated on the AW139, that is a highly successful civil helicopter, certified according to the latest flaw tolerance requirements. It is operated by many customers, with a wide and complex variety of different usage, and consequent spectra variability. Fig. 9 shows a statistical distribution of main usage and of the time spent in a specific mission. Optimizing the usage spectrum to cover all applications is a too conservative solution, that may cause some unnecessary penalties: therefore AW is working to improve the very few fatigue limitations or penalties in the Maintenance Manual to reduce costs per flight hour.

For this purpose, a HUMS system is under development for the AW139 helicopter, as already described in the last National Review. It includes:

- a Transmission Vibration Monitoring (TVM) unit, based on 11 accelerometers and 1 speed sensor;
- a Rotor Track and Balance (RTB) system, based on 4 accelerometers, 2 magnetic sensors and 1 tracking device;
- a Usage Monitoring (UM) system, subdivided into Structural (airframe and dynamic components) and Transmission (drive system) Usage Monitoring.

The long-term objective of this activity is to trigger a Condition Based Maintenance programme; the short- or medium-term objective is to tune in a rational way the replacement lives with the real usage.

As far as the fatigue life of MR blades is concerned, according to Usage Monitoring data (see Fig. 10) and customer service reports, the low cycle fatigue due to rotor Start-Stop and Ground-Air-Ground cycles is overestimated in the design usage spectrum.

AW is therefore implementing life limitations of blades in number of landing cycles, which is a countable event specific of the service usage of each helicopter. This is replacing the life limit based on flight hours only and the assumed worst case of rotor start-stop events.

A more comprehensive usage of HUMS data can further improve the Maintenance Manual, bringing to the reduction of life cycle costs.

2.7 - G222 Program (Alenia Aermacchi)

Due to new operative scenarios of the G222 aircraft, that has been partially refurbished, it has been necessary to evaluate the in-service usage in comparison with the design one, in order to evaluate the Life Severity Index and the Residual Life for the fleet, on the basis of the new mission profiles and mixing, due to the new aircraft usage.

An aircraft fatigue monitoring activity is being performed by means of classic mechanical g-meter readings and on the basis of provided information about configurations and mission profiles and mixing. The evaluation of fatigue consumption rate for each aircraft is based on the collection and analysis of the following flight parameters: Take-off weight, Fuel at Take-off, Fuel at Full Stop Landing, Number of Touch&GOs, Number of Full Stop Landings, Fatigue Meter strings. The fatigue damage is conventionally calculated at the wing root lower panel, which is a location that shows good sensitivity to all fatigue loads, both on ground and in flight.

The "Load Severity Index" is defined as the ratio between the In-Service Life Damage and the Design Life Usage.

$$LSI = \frac{\text{In - Service Life Damage}}{\text{Design Life Damage}}$$

The LSI allows to "convert" the in-service flight hours flown by each aircraft to the "equivalent" flight hours flown according to the design usage. The Design Life Damage is the fatigue damage calculated according to the design profiles and mixing, which were applied during the full scale fatigue test.

The Residual Fatigue Life, RFL, is evaluated as follows:

$$RFL = FLi - LSI * FH$$

where FLi is the initial fatigue life (measured in flight hours) of each aircraft, i.e. the design fatigue life that every component has at the beginning of the operative life, and FH are the flight hours flown by the aircraft. A typical fatigue-meter is shown in Fig. 11.

3. METALS

3.1 - Fatigue behaviour of notched and un-notched materials

3.1.1 - Evaluation of mechanical milling solutions instead of chemical milling (Alenia Aermacchi)

The processes improvement, the cost reduction and the more and more urgent time of production have been the push to take into account the introduction of mechanical milled fuselage skin panels in the ATR program, instead of the more traditional chemical milled panels.

Two processes have been evaluated: a traditional milling, performed following a standard procedure, and a new technology, "Mirror Milling". Mirror milling is a machining technique consisting in a mechanical milling performed through a cutting tool working on the item to be machined, operating by one side, with a dynamic local support on the opposite side that reacts to the cutting tool and, at the same time, provides a feedback about the exact position of the tool to the numerical control system (see Fig. 12 for a sketch). One of the main advantages of this technique consists in the possibility of avoiding the use of conventional support tools, that are replaced by the above mentioned dynamic support. The technique is mainly oriented to the manufacturing (pocketing) of fuselage panels, and can be considered as alternative/substitutive of the current chemical milling process.

An investigation has been performed to compare and evaluate the behaviour of typical fuselage skin panels manufactured by means of the two different production processes. For this purpose, simple coupons manufactured in 2024-T3 and 7075-T6 sheet have been tested, under Constant Amplitude load conditions. Different geometries have been evaluated, both from the point of view of geometrical accuracy and of the fatigue resistance.

The results showed some unexpected differences that required further investigation; a macro view of the geometry of a pocket shows that the geometry obtained with the chemical milling process is not as accurate as the one obtained by means of mechanical milling, see Figure 13; anyhow, the presence of a ramp is capable of improving the fatigue resistance of the chemical milled specimen with respect to the mechanical milled one.

An additional new coupon geometry has been defined, Fig. 14, and the results obtained confirm that mechanical milling is a valid alternative to chemical milling, both in terms of fatigue performance and geometrical accuracy. A 4 mm base radius gives acceptable performance in terms of fatigue life and so it will be the one chosen for production and certification testing.

3.1.2 - Fatigue behaviour of Inconel 718 coupons (Univ. Pisa)

Fatigue tests were carried out on Inconel 718 specimens in the framework of a cooperation between DICI (Department of Civil and Industrial Engineering - Univ. Pisa) and Agusta Westland. Seven groups of fifteen specimens were examined; Tab. I describes the test program, showing the differences of the various types of tests (grain direction of the specimens, Stress Ratio, Stress Concentration Factor and test temperature). Two geometries were considered: unnotched and notched ($K_t=3$), see fig. 15.

Fig. 16 shows some results of the activity; in particular, the results of the tests carried out at 400 °C, on Longitudinal and Transversal un-notched specimens are given, compared with the results of the tests carried out at room temperature on Longitudinal specimens. The stress ratio was $R=-1$.

The following conclusions can be drawn from the results given in Fig. 16:

- No appreciable differences exist between Longitudinal and Transversal specimens;
- The fatigue resistance of the material tested at 400 °C is higher than that at room temperature at high number of cycles, while it is slightly lower at low number of cycles.

As usual, fatigue cracks nucleated on the external surface; the only one exception was a Longitudinal specimen tested at 400 °C, in which a defect nucleated from the inside, fig. 17.

3.1.3 - Development of numerical simulation of the Laser Shock Peening process (Univ. Bologna)

Laser Shock Peening (LSP) is an emerging and promising technique to induce compressive residual stresses in fatigue critical metallic components. The LSP treatment produces mechanical shock waves due to the high pressure plasma (order of GPa) created on the treated surface, as a consequence of high-power density laser irradiation. The

surface itself is usually covered with an ablative layer (e.g. black paint or an extra thin layer of pure aluminium), over which runs a thin layer of water (tamping layer). The laser light pulse passes through the tamping layer and hits the ablative layer, which evaporates into the plasma state. The plasma expands rapidly, while the plasma-tamping layer reacting force causes a compression shock, that propagates into the metal.

The compressive residual stresses underneath the surface of the treated material are deeper than those induced by other more conventional processes, such as shot peening. In addition, LSP allows better accuracy and reproducibility, with smoother surface as a result, when compared with shot peening. The drawback of LSP is usually connected with longer surface preparation times and equipment costs.

Since LSP is a relatively young technology, most investigations have been concentrated on experimentally determining its mechanical effects, in order to optimize the combination of the metal and relevant LSP configuration that realizes the most appropriate residual stress field and the best surface morphology. These investigations are quite expensive, also for the sophisticated instrumentations required to evaluate the residual stress field and to measure quantities in a very quick process. A more rational approach is highly required, to drive in a more efficient way the selection/optimization of process parameters like: laser settings (energy density, pulse duration, number of layers); geometry of the target (thickness, shape, critical points like edges); laser peening sequence; environmental conditions (ablative layer, tamping coat).

A research activity is in progress at the University of Bologna - Forlì campus, with the aim to develop a new user friendly tool: the method is based on the commercial code ABAQUS. Furthermore, an extensive campaign of experimental tests has been carried out to calibrate the model and to verify the reliability in different peening conditions and for different target geometries. In order to achieve an optimized modelling time, the method has been developed using only the Explicit/ABAQUS code, allowing a one-step analysis. The Explicit code will, at the same time, guarantee the convergence even for the first "fast impact" phase.

Finite Element Model

The material chosen for the analysis is a 7050-T7451 aluminium alloy, representative of the experimental tests. Due to the high strain rate loading, the Johnson Cook's (JC) empirical material model has been used. The JC model describes the flow stress of the material as the product of three terms: one related with the strain hardening, another with the strain rate and a third one on thermal dependence. The JC equation is already implemented in ABAQUS/Explicit software: the user can directly input the values of the parameters without carrying out other specific procedures.

The high plasma pressure resulting from the high-energy laser pulse impact can be defined by a spatial and temporal profile. The pressure peak is dependent on the individual LSP conditions and a relation between the laser intensity (GW/cm²) and the pressure peak (GPa) can be found. For 1064 nm wavelength and 4 GW/cm² intensity laser, values representative of the experimental conditions, the peak pressure is about 3.5 GPa.

Mesh sensitivity studies have been carried out, in order to optimize the mesh; for this purpose, only the elastic material behaviour has been considered. Even if the plasticity effects are not taken into account, a non-linear distribution of stresses and displacements is present. This is a sort of "vibration" of the specimen due to the shock wave passing through it. Since the stress and displacement values must be zero at the end of the analysis, bulk viscosity coefficients were introduced in order to damp the vibration. The coefficients are merely numerical parameters available in ABAQUS/Explicit FE software, providing an artificial damping associated with the volumetric straining.

Numerical Results

A set of non-linear analyses with elastic-plastic material has been performed. The numerical results in terms of maximum displacement in direction perpendicular to the treated surface (11 µm) are very close to the experimental measurements (13 µm), as shown in Figure 18. However, the set of JC parameters is representative of a material with a very low yield strength, close to 80 MPa, far below the measured 469 MPa for standard Al7050-T7451.

Since the only parameter that influences the displacement field is the yield strength, it seems that the simulation does not take into account some aspects related to the surface condition (temperature effect, ablative layer). This result shows that the analysis must include a zone where the thermal effect is significant. It is therefore necessary to accurately model the ablative layer. A 100 µm thick layer of pure aluminium, with a yield stress of 10 MPa, has been simulated.

The final calibration of the numerical model has been carried out comparing the displacement and stress field with experimental results. As shown in Figure 19, the simulation of the ablative layer follows the experimental results trend, overcoming the underestimate of compressive displacement with the standard model. The comparison has been done with a 2-18-1 configuration, where the first number stands for laser power density in GW/cm², the second one the pulse duration in nanoseconds, the third the number of laser layers.

The modelling strategy previously optimized has been applied to more complex geometric configurations. The specimen geometry (Figure 20) has been defined after an intensive research campaign developed by Airbus in collaboration with EADS-IW. All the specimens have been sent to Metal Improvement Company (UK) for LSP treatment.

The performed simulations take into account the pure aluminium ablative layer. Several patches of laser spots have been overlaid on three faces of the specimen. Numerical results in terms of residual stresses have been compared with

experimental measurements carried out in EADS-IW. The results are shown in Figure 21 for 4-18-2 laser configuration. Two different reference paths have been taken into account.

More detail on this activity can be found in a paper presented at the Symposium, [1].

3.2 - Crack propagation and fracture mechanics

3.2.1 - Damage Tolerance evaluation of flat panels stiffened by bonded pads (Univ. Pisa)

Within the framework of a collaboration with Piaggio Aero Industries (PAI), an experimental program has been performed at the Department of Aerospace Engineering of the University of Pisa, aimed at assessing the fatigue crack growth and the residual strength of stiffened panels with bonded pads.

A couple of nominally identical flat panels were tested, external dimensions 1470 x 1200 mm, stiffened by means of 5 bonded pads with a C shaped (height 50 mm, width 20 mm) cross section stiffener riveted on the central pad (width 28 mm). The panels were made by bonding 2024-T3 pads onto a 0.8 mm thick skin of the same material. The panels had an initial through crack in the central pad (and in the skin underneath) and the stiffener was severed.

The dimensions of the test articles were the same of pad stiffened panels previously tested to assess the effectiveness of the pads as crack stoppers. Due to the small height-to-width ratio of the panels, the gripping plates specifically designed to carry out the previous activity were used in order to obtain a stabilized stress distribution in the central region of the panel, which is the location of interest. Fig. 22 shows some photos illustrating the test set up.

Due to the presence of the stringer on one side, secondary bending is unavoidable; consequently, guides with Teflon pads (to minimize the effects of friction) were installed on the frame of the testing machine in order to restraint the out-of-plane displacements of the stringer in the vicinity of the crack initiation area. Crack propagation was visually monitored on both sides of the panels through optical microscopes (see Fig. 22) to evaluate potential effects of secondary bending.

For the fatigue crack growth test, the panels have been subjected to a constant amplitude cyclic load, characterized by a maximum average stress level of 90 MPa and a stress ratio $R = 0.1$. After completion of the fatigue crack growth test (i.e. when a two bay crack was reached), a residual strength test was performed for each panel.

The results of the crack propagation tests on the two panels are summarized in Fig. 23. Analyzing these results, the following observations can be made:

- The crack propagation life of panel 1 is quite shorter than the one of panel 2;
- Crack propagation rates are comparable when the crack is propagating in the skin;
- Crack propagation rates differ significantly when the crack is propagating in the pad but they are comparable when the crack is propagating in the skin only.

Secondary bending effects are limited, as demonstrated by the results shown in Fig. 24 in which crack propagation measured on both sides of the panel are compared. Very small differences are visible only as long as the crack propagates in the central pads while they vanish as soon as the propagation interests only the skin.

The results of the residual strength tests on the two panels are summarized in Fig. 25 in terms of mean gross stress to maximum cyclic load ratio vs. half crack length increase.

The half crack length increase has been measured from digital frames, captured by a video camera, using a graduated scale traced on the test articles for this purpose. The mean gross stress has been derived dividing the measured load by the cross sectional area of the whole panel (undamaged stringer, skin and multilayered pads).

Data in Fig. 25 shows that the test articles underwent a stable crack propagation phase of different duration; the failure stress was always higher than twice the maximum stress applied in the fatigue crack propagation phase.

3.2.2 - Damage tolerance characterization of Mg cast alloys (AgustaWestland)

Application of Mg alloys in cast components (e.g. transmission case) is of great interest in the helicopter industry. AgustaWestland is continuously updating the materials data base with respect to fracture mechanics and flaw tolerance properties, and in the last two years the Mg cast alloys Elektron 21 and ZE41 have been evaluated, in collaboration with the Polytechnic of Milan - Department of Mechanical Engineering. Fatigue S-N properties were evaluated in AW laboratories in Cascina Costa. Fig. 26 shows $da/dN - \Delta K$ results for Elektron 21 magnesium alloy.

It may be interesting to quote that also F357, a "berillium free" aluminium alloy likely to substitute the widely used A357 for casting elements, has been evaluated in terms of Fracture Mechanics properties.

4. COMPOSITES AND FIBER METAL LAMINATES

4.1 - A novel cohesive zone modelling approach to evaluate Damage Tolerance of composite laminates (Milan Polytechnic)

The basic principles of this innovative approach were already presented in the last National Review. In the last two years, refinement and tuning of the analysis methodology have been carried out, by means of comparison with a number of experimental results, generated by tests performed on different coupons or structural elements, made of various materials. The accuracy of the method prediction depends on a number of parameters that have been tuned, for a graphite system and for a glass/epoxy system of common usage in the helicopter industry, thanks to a wide test activity.

As an example, curved beam specimens, tested in 4-point bending and in tension, experience multiple delamination during the failure process; identification of the critical interfaces and prediction of the damage progression is a very difficult task, that has been successfully overcome by the analysis method.

In a similar way, also simple interlaminar fracture mechanics coupons, such as DCB and ENF, have been modelled, obtaining a very faithful correlation with the experimental results, even in the presence of fiber bridging in mode I test. Dedicated tests, aimed at collecting a vast amount of information (it may be significant to quote that also strain measurements were carried out, by means of embedded FBGs), were performed, to obtain a specific R-a curve. A non-linear cohesive law can be used in these cases, which can be approximated by means of two superimposed linear laws. More details on this last specific topic can be found in [2], while most of the activity has converged in a paper to be presented at the Symposium, [3].

4.2 - Interlaminar Fracture Mechanics characterization of composites (Univ. Pisa)

In the previous National Review, a paragraph was dedicated to the start of a collaboration between AgustaWestland and the former Department of Aerospace Engineering of the University of Pisa (now DICI, Department of Civil and Industrial Engineering) with the objective of characterizing a few composite material systems as far as their fatigue and delamination resistance is concerned. The activity started with two carbon fibre systems: a fabric 5H 8552S/AGP280 and a unidirectional 8552/AS4. In the period of this Review, two more systems were added: a glass fibre Cytec S2-5216 and a graphite/epoxy system, Hexcel 913C-HTA.

For each of them, static tests to evaluate the mode I, mode II and mixed mode I+II (with two different values of the mode partition ratio) G_c have been performed. Three batches of specimens have been manufactured for mode I (DCB coupons) and mode II tests (ENF coupons), to cover adequately the scatter in the properties.

Moreover, also fatigue curves, again on three batches for the pure mode I and II conditions, have been performed to evaluate the number of cycles for delamination onset. A criterion of 5% stiffness decrease has been selected for these tests. For the mode II fatigue tests, a pre-crack has been introduced, to avoid over conservative results. As an example of this type of results, Fig. 27 shows a normalized G_{max} vs. cycles curve for mode I delamination onset resistance, for the glass/epoxy S2-5216 system.

Most of the experimental results have been used in a collaboration with Milan Polytechnic to calibrate and tune a new model based on a hybrid FE approach that allows the use of cohesive laws in a simple manner. More details can be found in a paper presented at the Symposium [3].

5. COMPONENT AND FULL-SCALE TESTING

5.1 - Development fatigue test of M-346 components (Alenia Aermacchi)

This test was anticipated in the last National Review, where preparation activities were described; in the last two years, the test has been successfully completed. The objective of this test was to investigate the behaviour of the cabin floor made in CFC in presence of defects positioned in the critical “T” section of the item (i.e. the section where is the joint with skin, Fig. 28).

The test was a “development test” because the floor was produced by means of a “prototypical” manufacturing process, the main issue of which was the generation of some “defects” in the filler of “T” section (similar to “voids”) and which therefore was afterward improved. Moreover, in the subsequent series configuration, the geometry of the critical section was slightly modified.

The test article was only a portion of the cabin floor, i.e. one of the “T” sections and the prolongations of the other section were cut off. The “T” section under analysis was fixed to a beam representing the front fuselage lateral skin and frames as it is on the aircraft, Fig. 29. The floor is supported by two tubes that represent the nose landing gear longerons.

The simulated loads were only the pressurization ones, being the pressure cycles the most significant fatigue cycles applied to this item. The loads were applied by means of 5 pads in the direction perpendicular to the floor and by means of 8 plates clamped to the structure in the direction parallel to the floor, Fig. 29; this load set-up simulated the

stress/strain state at the “T” section. The loads were applied in a flight-by-flight sequence, i.e. a sequence that resembled the random sequence of missions and the mission pressurisation profiles. Before the start of the test, the test article was conditioned at 75 °C and 85% RH.

The fatigue test was conducted to accumulate 20000 TFH, at room temperature. Moisture loss was monitored by means of the specimens that were conditioned together with the test article, to check the conditioning status before the start of the fatigue test.

During the test, NDI inspections were periodically performed to monitor the defects status. After application of two lifetimes load sequence, a Residual Strength static test has been performed at UL (at room temperature). Despite the test article conditioning, considering the design temperature effects and the humidity lost during the test, an additional 1.15 factor has been used to increase the loads.

During the fatigue test, the defects have grown, but nevertheless the test article resisted to the ultimate load (for 3 seconds) without collapsing, i.e. it demonstrated a satisfactory residual strength.

The development test, even if applied to a “prototypical” configuration due to the manufacturing process modification, was nevertheless important and useful in order to evaluate the general structural capability of the cabin floor and its resistance to embedded defects.

At the moment, with the manufacturing process stabilised for the series production, the defects that were found in the test article are no more present; therefore, the series configuration of the CFC cabin floor is going to start another test (similarly to the “prototypical” configuration) with artificial defects inserted at the critical “T” section.

5.2 – M-346 certification Full Scale and component fatigue tests (Alenia Aermacchi)

Some information on these tests was already given in the last National Review; now they are in progress and more recent information on their status is given in the following.

The Full Scale Fatigue Test (FSFT) is carried out on a test article that comprises the fuselage and the wings, including the leading edge flaps (i.e. nose droops), but not the trailing edge flap and the aileron, that will be separately tested on a dedicated rig, as well as the vertical and horizontal tails. The loads introduced on the test article by these components are applied using suitable dummies/tools or directly by actuators acting on their attachments. In particular, engines, tailplanes and landing gears are simulated by means of dummies.

The loads are introduced basically by means of actuators. In particular:

- the loads applied to the wing box are introduced by actuators interfaced at the pylons attachment points (4 stations), see Fig. 30;
- the loads applied to the leading edge surfaces are introduced by whiffle trees joined to the structure by means of bonded pads;
- the loads applied to the fuselage are introduced by whiffle trees and stand-alone actuators;
- the loads introduced by tailplanes are applied through the dummies, see Fig. 31;
- the loads introduced by wing trailing edge surfaces are applied through the dummies and directly by actuators, see Fig. 30.

In total, 62 loading points are present on the test article. The locations and the applied forces have been evaluated with the aim to simulate as closely as possible the design internal forces and moments distribution (shear, bending and torsion moments) on the aircraft structure and to generate null (or negligible) resultants at the dummy landing gears constraints.

Once the test loads have been defined, the equivalent damage approach is applied in order to evaluate, at a selected number of control points, the “test” damage and to compare it with the “design” damage; the first one should be greater than or equal to the second one. With these two values, the severity index at the control points is calculated, a parameter necessary to convert the “tested flight hours” into the “design flight hours”.

Control points are identified as the sections

- with lowest lives;
- with intrinsically criticality from the structural standpoint (e.g. single load path elements);
- with criticality due to the concentrated test loads application.

The loads are applied by means of a flight-by-flight sequence that is nevertheless simplified with respect to the one used for fatigue calculation under design loads and spectra; conditions that give negligible contribution to the damage accumulation (but occur a high number of times) have been eliminated, while, on the other end of the cumulative diagram, the occurrences of other conditions that produce a significant damage have been increased. Moreover, cabin pressurization cycles are applied following the mission profiles, i.e. superimposing pressure loads to manoeuvre/gust loads during appropriate mission segments.

Ground segments are also simulated and applied at the dummy landing gear interfaces. In this case, the aircraft structure is appropriately loaded in order to have resultants at the dummy landing gears constraints equal to the ground loads.

Finally, also “dynamic” loads, due to the buffet phenomenon, are introduced into the test article. Being this phenomenon significant for the tailplanes, the rear fuselage structure at the interface with the vertical and the horizontal tail shall be tested under buffet loads.

The approach used to introduce buffet loads is “quasi-static”, i.e. the loads are introduced by actuators through the above-described dummies. The options selected for HT fatigue test (i.e. use of shakers to excite the structural modes) or in the VT fatigue test (i.e. to introduce Power Spectral Density load profiles) has not been considered feasible for the complete aircraft. Moreover, as far as the rear fuselage is concerned, the structural components affected by these spectra are just those at the surface interface, i.e. the most important issue was to resemble as much as possible interface loads, rather than simulate the dynamic behaviour of the entire structure, which, on the other hand, is the main issue for the tailplanes “buffet” fatigue test. At the end of the procedure above-described, two main load spectra (that from now on can be called “blocks”) are defined:

- Static block (manoeuvre and gust plus pressurization, ground loads)
- Quasi-static block (HT and VT buffet)

Each block represents 500 TFH (tested flight hours). The buffet block is subsequent to the static one.

At February 2013, the test has accumulated 2000 TFH and a further sequence of 1000 TFH is almost finished. The goal of the test is to accumulate two durability lives (20000 TFH).

Periodically visual and non-destructive inspections are performed to check the structural integrity of the test article. Up to now, no evidence of cracks has been found.

5.2.1 M-346 Horizontal Tail (HT) Fatigue test

The M-346 horizontal tail is tested on a separate rig from the FSFT. The test article comprises not only the aerodynamic surface, but also a dummy actuator with the corresponding lever and mount, which altogether represent the horizontal tail actuation system.

Two main load sources are applied to the HT: “static” loads, i.e. loads derived from manoeuvre and gust events, and “dynamic” loads, i.e. loads derived from the buffet phenomenon occurring at high angle of attack.

“Static” loads are applied by means of actuators (8 actuators that introduce the forces through 4 saddles, Fig. 32) that act perpendicularly to the tail mid plane. The theoretical distribution of aerodynamic and inertial loads is discretised into concentrated loads with the aim to reproduce the internal actions as closely as possible (Fig. 33).

Also in this case, “control points” have been identified to assess the severity index, i.e. the ratio of the “test” damage to the “design” damage; the first should be greater than or equal to the second. The severity index at the control points are used to convert the “tested flight hours” into the “design flight hours”. The loads are applied by means of a flight-by-flight sequence.

“Dynamic” loads application is more complicated as buffet effects are superimposed to manoeuvre conditions, therefore the complete dynamic condition is composed by a “mean” value, due to the manoeuvre that the aircraft is performing, and an “alternate” value, that is the contribution of the buffet that is triggered during the manoeuvre. When the mean static component is negligible with respect to the dynamic alternate one, the load condition can be assimilated to a “pure” dynamic load; on the other hand, if the mean static component is significant, the superimposition of the two shall be simulated. As far as the HT flight-by-flight load spectrum is considered, both the above-described scenarios are present and therefore two different approaches have been applied to deal with buffet loads.

Whichever approach is applied, first of all a mode reduction is performed, i.e. the contribution to the total damage of each mode that is analytically considered for buffet damage calculation is evaluated; the normal modes that give a negligible contribution to the damage accumulation are removed from the test spectrum definition procedure. This process is necessary, otherwise the load application on the test article would be problematical, if not possible at all.

The first approach is similar to the application of static loads and is applied when the mean static component is not negligible. The actuators mentioned before are used to apply “quasi-static” conditions that are derived from the buffet loads added to the manoeuvre ones. The same approach for force distribution and damage calculation is applied.

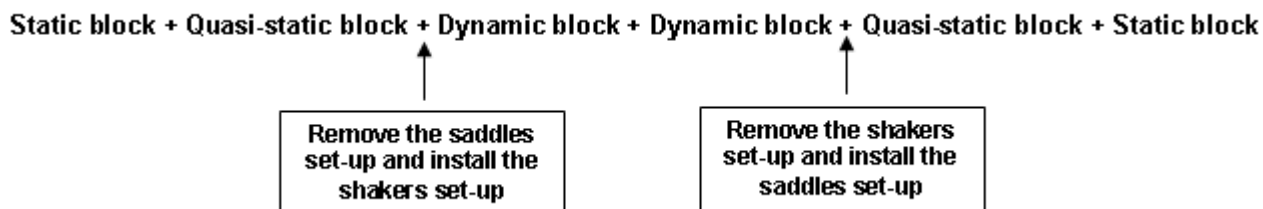
The other approach, applied when the mean static component is negligible, is completely different, as the loads are applied to the structure by means of two shakers. The shakers excite the normal modes mainly involved during the buffet phenomenon by means of sinusoidal loads. Therefore the dynamic response of the HT shall be monitored throughout the test duration because even slight frequency modifications can largely affect the dynamic behaviour of the test article and therefore the simulation of the buffet phenomenon. Apart from the different method of load application, test spectrum definition is nevertheless performed applying the equivalent damage approach.

The portion of the flight-by-flight spectrum, to which either the quasi-static or the dynamic approach is applied, is defined by means of a mission segment analysis. Since the missions and the mission segments during which the buffet phenomenon is triggered (due to the Mach, altitude and angle of attack conditions) are known, the influence of the “mean” static load component on the total damage is evaluated for each of them. The result of this evaluation is that only for few mission segments and manoeuvres the mean static component cannot be neglected and therefore the quasi-static spectrum is defined only for these few cases.

At the end of the procedure above-described, three load spectra (“blocks”) are defined:

- Static block (manoeuvre and gust)
- Quasi-static block (buffet)
- Dynamic block (buffet)

Each block represents 500 TFH (tested flight hours). In order to have a compromise between the concept of random flight-by-flight spectra and the opportunity of reducing time and cost, the sequence of block application is the following:



The above sequence represents 1000 TFH.

At February 2013, the test has accumulated 3000 TFH and the subsequent sequence of 1000 TFH is in progress. The goal is to accumulate two durability lives (20000 TFH). Periodically visual and non-destructive inspections are performed to check the structural integrity of the test article. Up to now, no evidence of cracks has been found.

5.2.2 M-346 Vertical Tail (VT) Fatigue test

Also the M-346 vertical tail (VT) is tested on a separate rig. The test article comprises not only the fixed and mobile aerodynamic surfaces, i.e. fin and rudder, but also a dummy actuator with the corresponding lever and mount, which altogether represent the rudder actuation system. Two main types of loads are applied to the surface: “static” loads, i.e. loads derived from manoeuvre and gust events, and “dynamic” loads, i.e. those derived from high angle of attack and airbrake deployment buffet phenomenon.

“Static” loads are applied by means of actuators (14 actuators that introduce the forces through 5 saddles on the fin and 4 pads on the rudder, Fig. 34 and 35) that act perpendicularly to the surface mid plane. Also in this case, the equivalent damage approach has been applied and the severity index evaluated in a number of control points. The loads are applied by means of a flight-by-flight sequence.

When buffet is triggered, the mean static component is negligible and so “dynamic” loads are applied by means of two shakers (see Fig. 36). The shakers apply to the structure a Power Spectral Density (PSD) load profile that resembles the actual loading acting on the VT during the buffet phenomenon. By means of this approach, buffet experimental simulation is not sensitive to VT dynamic response; nevertheless the latter is monitored throughout the test duration with the main purpose of evaluating how much continuous dynamic excitation affects the structure behaviour. Apart from the different method of load application, dynamic test spectrum definition is nevertheless performed applying the equivalent damage approach.

At the end of the procedure above-described, two load spectra (“blocks”) are defined:

- Static block (manoeuvre and gust)
- Dynamic block (buffet)

Each block represents 500 TFH (tested flight hours). The goal is to accumulate two durability lives (20000 TFH).

At February 2013, the test has accumulated 1000 TFH because it has been stopped due to a finding during a scheduled inspection. Two cracks were identified at the interface between the top rib and the V/HUF antenna. The section is highly stressed during the airbrake deployment phases that trigger the buffet phenomenon and in fact its criticality was highlighted also by the analytical evaluations; the criticality and its source were confirmed as the section was inspected after the static block application and no cracks were found, while they appeared during the buffet block. After a first repair with the purpose of going on with the test until a new structural configuration had been designed, the test has been stopped in order to introduce the re-design in the test article. This new design solves the fatigue issues connected to the buffet phenomenon. Up to now the retrofit is completed and the test setting is almost terminated, so that the test can start again soon.

In the meantime, a more detailed evaluation about the airbrake buffet spectrum applied to the test has been performed, as it was derived from a prototype airbrake deployment schedule; the series (i.e. final) deployment schedule has been checked to be much less severe, and this makes the new structural configuration even more solid and durable.

5.2.3 M-346 outer nose droop balance Damage Tolerance test

This item represents the interface between the outer nose droop (i.e. leading edge flap) and its actuator installed on the wing box. Since it is a single load path with a high structural criticality, a dedicated test on a fixed rig has been

developed. Moreover, the criticality is related mainly with the damage tolerance requirement (i.e. crack growth issues); the test was designed with the aim to check the compliance with such requirement. Nevertheless, in this test, similarly to all the damage tolerance certification tests, 2 lifetimes are applied before the damage tolerance demonstration, in order to show also adequate durability qualities.

A sketch of the rig is shown in Fig. 37. One actuator applies the load through a tool that reproduces (for what concerns geometry and stiffness) the lug interface at the leading edge side. The balance is linked to the rig representing the actuator by means of two rods that react the applied load (the rods are the real ones, used on the aircraft, but are here considered as tools, i.e. they are not under test).

The loads are applied by means of a flight-by-flight sequence that resembles the one used for fatigue calculation under design loads and spectra; actually, two sequences have been defined, one for the durability test and one for the damage tolerance one. The choice is due to the different approaches used to define the test spectrum: for the durability requirement, the equivalent damage approach is applied, therefore the design flight-by-flight sequence is simplified eliminating the conditions that give negligible contribution to the damage accumulation (but occur several times) and increasing the occurrences of other conditions that produce a significant damage. On the contrary, for the damage tolerance requirement, the goal in defining the test spectrum was to reproduce the crack growth in the most critical point of the balance, therefore loads are omitted only if the crack propagation curve under the test spectrum resembles the one under the design spectrum.

At February 2013, the test has accumulated 10000 TFH, i.e. one durability life, and application of the second durability life is now in progress. After the first life, visual and non-destructive inspections have been performed to check the structural integrity of the test article; no evidence of cracks has been found. At the end of the second life, a corner crack will be introduced in the most critical balance section and crack wires will be installed to monitor the crack propagation.

6. AIRCRAFT FATIGUE SUBSTANTIATION

6.1 - Development of the Bombardier C Series (Alenia Aermacchi)

Within the framework of this programme, focused on the design of a narrow body, medium range twin engine aircraft, Alenia Aermacchi is in charge of the Design and of the Fatigue/Damage Tolerance Analysis and Certification of Horizontal and Vertical Tail Structures.

In addition Alenia Aermacchi is in charge for Static and Fatigue Test development for material, structural details, component characterization and Full Scale Tests on horizontal and vertical tails.

The standard Building Block approach has been followed to characterize material, design choices and methodologies. Alenia Aermacchi is in charge also of the performance of the test activity to generate material allowables, as well as the assessment of the environment sensitivity and of the scatter. Moreover, also the Load Enhancement Factor that will be applied in the Full Scale Fatigue Test will be assessed, as a function of the scatter parameters of the Weibull distribution. Alenia Aermacchi has defined also all the progressively more complex structural elements included in the test pyramid, that will be manufactured and tested. Some tests have already been performed, as shown in Fig. 38.

The Full Scale Fatigue Test will be carried out in the Pomigliano Laboratory and the standard procedure outlined in Fig. 39 will be followed.

6.2 - AW 109 Helicopter family (AgustaWestland)

The AW109 LUH (Light Utility Helicopter, a military helicopter with a 3175 Kg AUW and a Vne of 140 Kts up to 20.000 ft altitude) is being analysed for extended Take Off Weight, increased at 3300 Kg, with a new limited flight envelope and loads to match requirements of South Africa client and new future bids.

The civil certification of A109SP (with a 3175 Kg AUW and a Vne = 168 Kts up to 20.000 ft altitude) at very low operating temperatures (- 40 °C OAT, Outside Air Temperature) was based on dedicated cold trials in Alaska (USA). The minimum OAT could significantly change rotor blade loads, due to the increased air density, and therefore also the Mach number at Main Rotor Blade tip; moreover, the stiffness of the elastomeric bearing could increase, as well as the associated loads to achieve required blade pitch.

The fatigue life management of MR Blades for various models of the family (AW109S, AW109SP and AW119) was modified, passing from a flight hour limit to a combined limitation based on flight hours and start-stop cycles, whichever limit is achieved first. This approach allows a better exploitation of the true blade fatigue lives, improving a closer matching of aircraft usage by different civil customers; each customer is typically characterized by a specific mixing of short and long flights, which is associated with a different spectrum severity.

6.3 - EH101 / AW101 Helicopter family (AgustaWestland)

The AW101 has a very demanding usage in severe environments and customers develop new requirements which require fatigue assessment. A few examples are listed in the following.

The Japan Navy was supported for evaluation of a customized Anti Mine Counter Measure mission.

A few military fleets, such as DMRH (Denmark), CSH (Canada) and Portugal, provided usage data of their HUMS systems to check the 'true' usage spectrum effectively flown, versus the assumptions agreed for fatigue analysis of their Maintenance Manual (MM) at the design stage. The usage evaluation was carried out; the way ahead is still to be decided. Other fleets are strongly interested in the exploitation of this powerful tool.

Operational Data Recording (ODR) of UK Merlin fleet was carried out by direct instrumentation of some relevant structural components in service environment. The parts instrumented included rotating components, rotor controls, transmission support, tail unit and tailplane; moreover, power spectra have been completely recorded in terms of applied couple and engine RPM. About 300 hours were recorded for 5 aircrafts, covering the two variants, Navy and Air Force. These data allowed the verification of the fatigue spectrum used for fatigue life calculations, in terms of both loading amplitude and occurrence. Also in this case, the way ahead and data exploitation are in progress; there is an obvious interest in evaluating if the design spectrum is consistent with the flown spectrum, due to the high costs associated with the main transmission maintenance.

SAR (Search And Rescue) version for Algeria and VVIP variants for Saudi and Turkmenistan required an improved fatigue analysis considering the full usage at 15.600 Kg AUW and $V_{ne} = 150$ Kts.

These variants and the outstanding performances for 'Skyfall' and Olympic Games are the latest involvements of AW101.

At present, two contracts are in progress: a CSAR version for the Italian AMI and a MLSP variant for the UK. They will account for dedicated usage, with NOE, air-to-air refuel and shipborne loads for the new articulated tail rotor.

6.4 - AW189/ AW139 / AW169 Helicopter family (AgustaWestland)

AgustaWestland has developed the concept of helicopter family: using the commonalities it is an efficient method to grow the number of models required by the market. The very successful model AW139 has therefore a bigger brother (AW 189, 8300-8600 Kg AUW) and a smaller brother (AW169, 4400 Kg AUW). In the following, some information is given about the two programs.

The AW189 is a new helicopter, the elder brother of the AW139 family, with a 8300-8600 Kg AUW, that is being certified this year with EASA. Its expected usage is: offshore, SAR, transport and cargo.

Four prototypes are flying and were supported in the last two years with monitoring and fatigue tracking for flight envelope investigation. Fatigue lives of prototypes were then computed according to their planned usage and specific trials were monitored in real time.

Fatigue safe lives are provided for all components, supplemented by mandatory inspection plan for all PSE (Primary Structural Elements) including all rotor parts, rotor controls, transmission shafts and gears.

Periodic review of test results, analysis and fatigue lives evaluation is in progress with EASA specialists for all the mechanical parts. Airframe tests are starting and an initial limited clearance is envisaged at present, according to the fuselage tests progresses.

AW169 is a new model, the smallest of the family AW189 - AW139 - AW169, with about 4400 Kg AUW.

Full development is in progress and EASA type certificate is expected by 2014. Two prototypes are flying at present plus a ground test vehicle. Fatigue activities are related to:

- monitor and tracking of prototypes flight activities;
- safe life tests and analysis;
- starting all the flaw and damage tolerance evaluations of mechanical parts.

Airframe structure fatigue and damage tolerance testing is being planned in details and the test rig and test article are in the manufacturing phase. Structural element tests have already started. Preliminary load survey is already available and full envelope is planned within summer 2013.

6.5 - AW139 helicopter LIPS demonstration (AgustaWestland)

In February 2010 the AW139 FIPS (Full Ice Protection System) was certified by EASA; it was the first civil helicopter of relatively small size (6 tons) to have this kit. From the structural point of view, the major consequences of FIPS are that the MR blades are equipped with a de-ice system to remove periodically ice accumulated on the blades themselves and the TR Blades have an anti-ice system preventing ice formation by blade heating.

More recently, an interest to demonstrate also LIPS (Limited Ice Protection System) capabilities was shown by some operators; LIPS is the capability to fly safely in icing conditions without Full Ice Protection System (FIPS). The clearance is defined in terms of parameters readily available to the crew. An activity related with the demonstration of AW139 capabilities for LIPS was performed and EASA certification is expected in a short time.

Ice accretion and increased drag and power required, modified loadings, ice shedding effects are the issues to be evaluated for fatigue and damage tolerance assessment.

The flight limitations are based on:

- **LWC** (Liquid Water Content); conditions are established for permitted continuous operations and more severe icing conditions for a limited period of flight, allowing safety margins to exit out of the cloud;
- **OAT** (Outside Air Temperature); the lowest temperature achieved during validation test, but not lower than -10°C ;
- **Time in ice**; time in which the aircraft can be operated in safe flight;
- **Airspeed**;
- **Altitude**;
- **Ice Accretion**.

6.6 - AW 609 development (AgustaWestland)

AW609 is the civil tilt-rotor developed by AgustaWestland from the past joint venture with Bell Helicopter. Fatigue tasks in these two years were focused on acquisition of the relevant data developed in the past by BHTI and on fully supporting the prototypes activities.

Full development activities are becoming progressively more relevant:

- Harmonization of methodologies with FAA;
- Material data bases for metal, composites and damage tolerance;
- Improvement of some development configurations;
- Development of fatigue test plans;
- Load survey requirements;
- Usage spectrum definition.

6.7 - UAS Technology (Alenia Aermacchi)

The NATO-STO-AVT-174 Working Group has been focused to the development of guidelines on Structural Design and Qualification for Unmanned Military Air Vehicles.

Having considered the increasing interest in design and production, together with the next future perspective of a large and “less restricted” use of UAVs, the group reviewed all structural design and qualification aspects. Starting from the consolidated approach adopted for conventional aircraft, focus has been put on peculiarities belonging to UAVs. This led to the production of a document, that proposes a summary of rules and practices deemed appropriate for UAVs to ensure an equivalent level of safety with respect to manned aircraft.

A new classification of Unmanned Vehicles categories has been proposed, on the basis of fatal risk of impact.

Alenia Aermacchi contribution has been focused on Durability and Damage Tolerance issues, and on their relevant Structural Qualification aspects.

The Group concluded its activities at the end of 2012 and the final report “Structural Design Criteria / Qualification Guidelines for Unmanned Military Air Vehicles” is foreseen by mid 2013.

7. REFERENCES

- [1] E. Troiani, C. Crudo, G. Molinari, S. Taddia: “Investigation on Laser Shock Peening Capability by Finite Element Simulation”, paper to be presented at the 27th ICAF Symposium, Jerusalem, 5-7 June 2013.
- [2] A. Airolidi, C.G. Davila: “Identification of material parameters for modelling delamination in the presence of fibre bridging”, *Composite Structures*, Vol. 94, issue 11, Nov. 12, pp. 3240-3249.
- [3] A. Airolidi et al.: “An Improved Methodology for the Design of Helicopter Structures in Composite Materials”, paper to be presented at the 27th ICAF Symposium, Jerusalem, 5-7 June 2013.

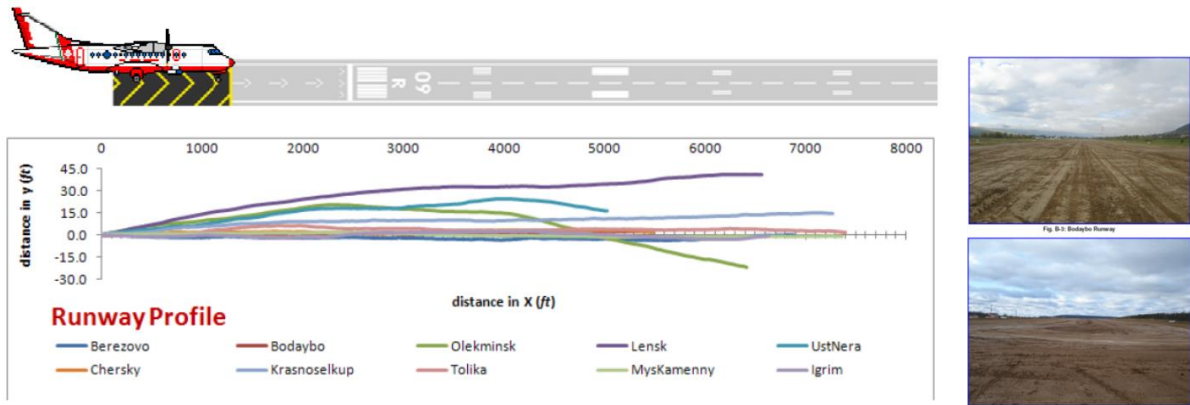


Fig. 1 - Profiles of the main Russian semi-prepared runways.

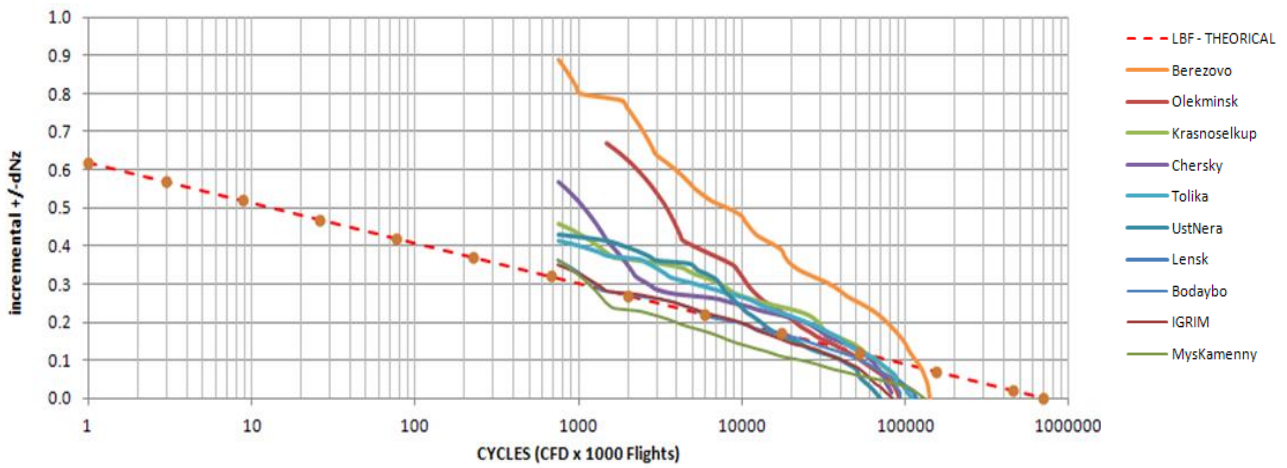


Fig. 2 - Cumulative Frequency Distributions of vertical acceleration increments, for various Russian semi-prepared runways.

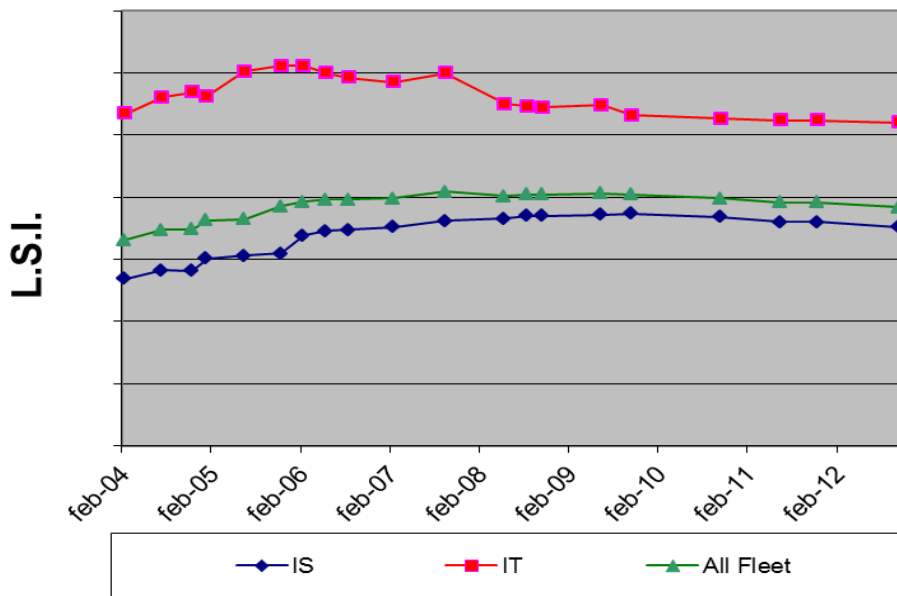


Fig. 3 - Load Severity Index distribution for the AM-X fleet (IS = strike; IT = trainer).

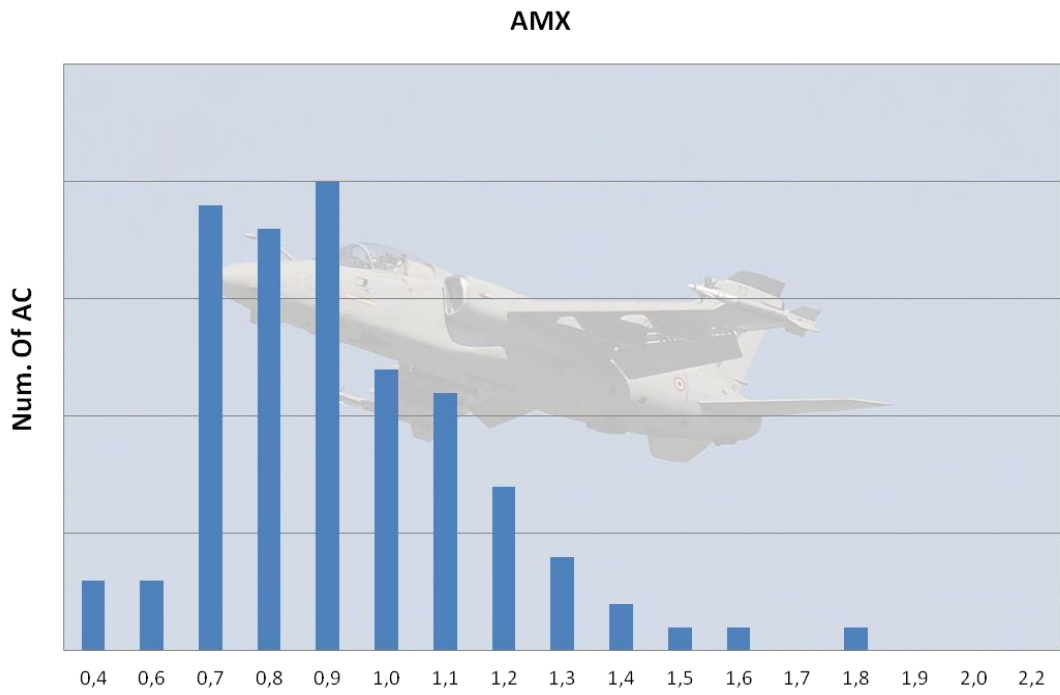
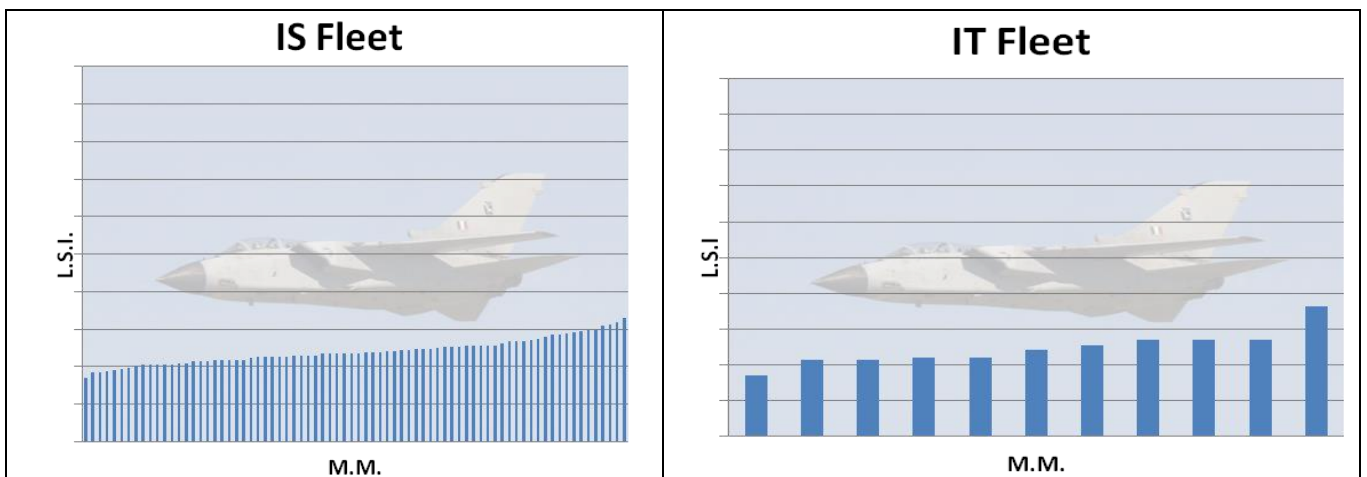


Fig. 4 - Load Severity Index distribution in the AM-X fleet.



**Fig. 5 - Load Severity Index distribution for the I.A.F. Tornado fleet.
(IS = strike; IT = trainer)**

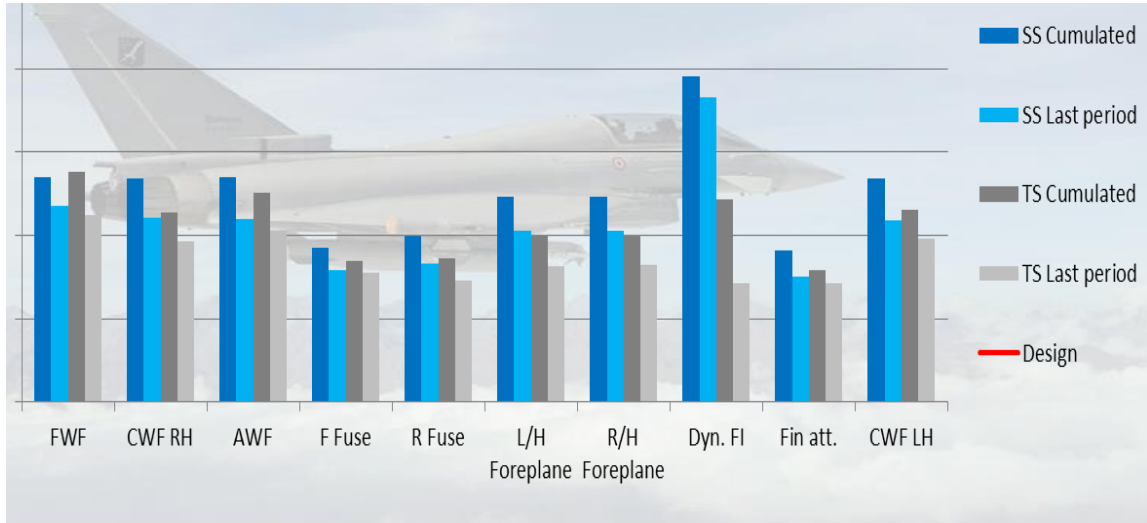


Fig. 6 - Fatigue Indexes values for IAF Typhoon aircraft. (SS = Single Seat; TS = Twin Seats).



Fig. 7 - FOBG instrumentation of a AW109SP prototype baggage door for evaluating the sensor system.

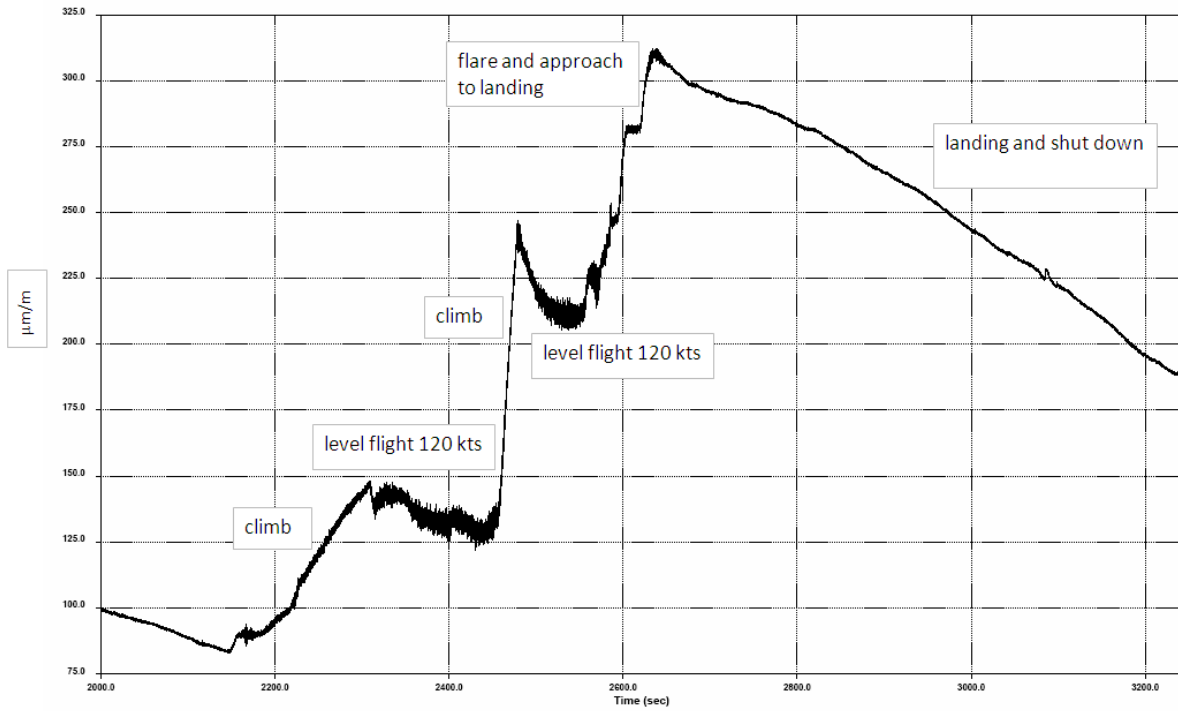


Fig. 8 - Strain vs. time history collected by FOBG instrumentation in a flight.

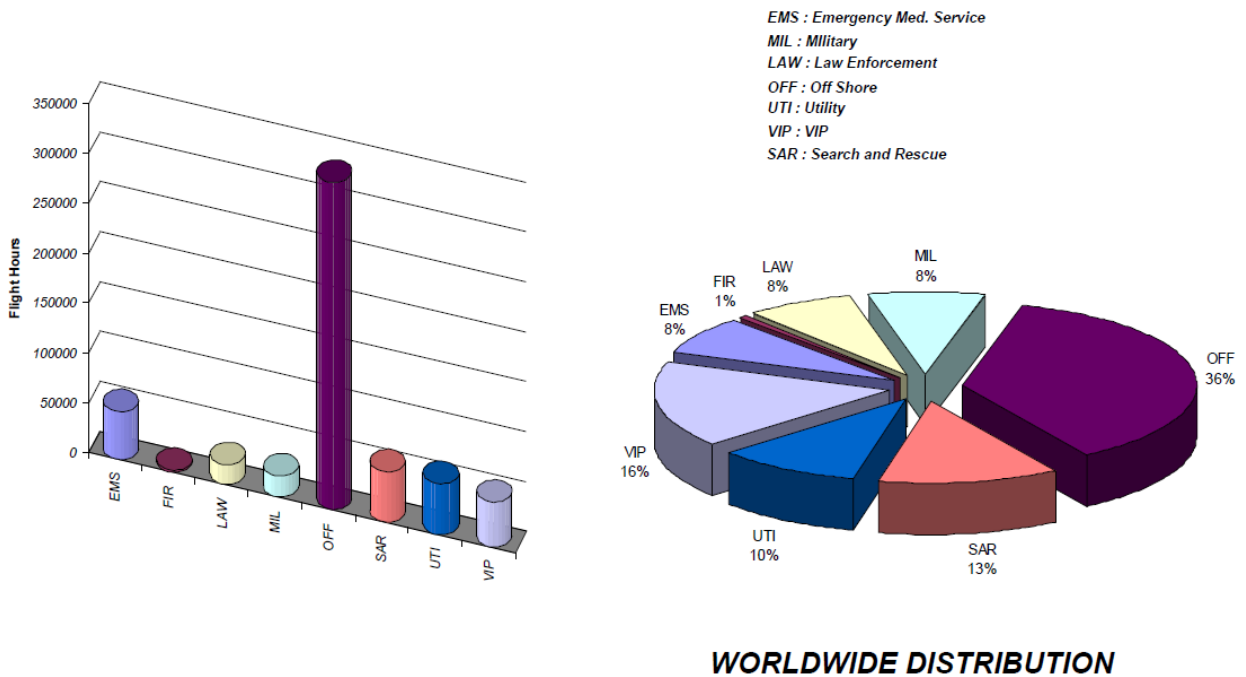


Fig. 9 - Distribution of the different missions performed by AW139 operators.

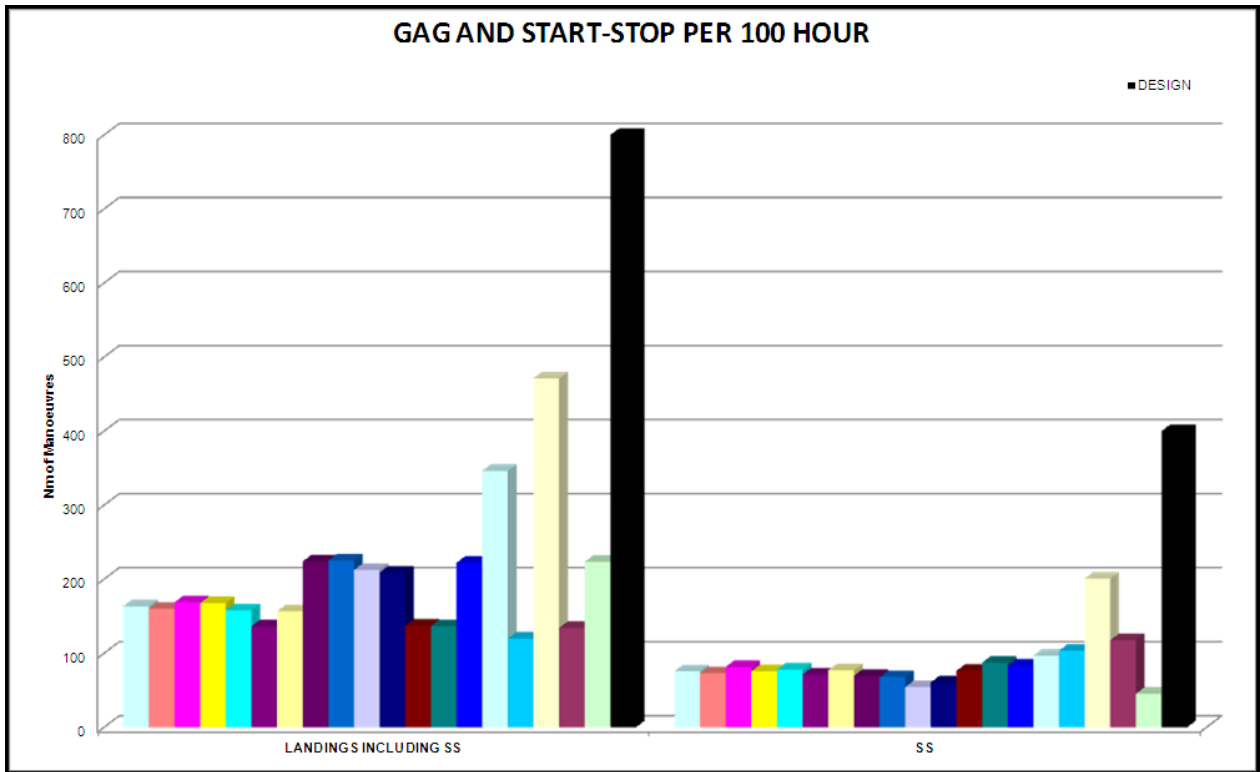


Fig. 10 - Distribution of the Start-Stop and of the Ground-Air-Ground cycles in the AW139 fleet.



Fig. 11 - Typical fatigue meter, used on the G222 I.A.F. fleet.

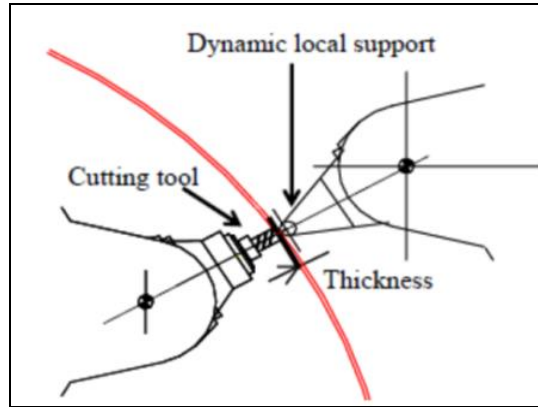


Fig. 12 - Sketch of the Mirror Milling technique for milling thin sheets.

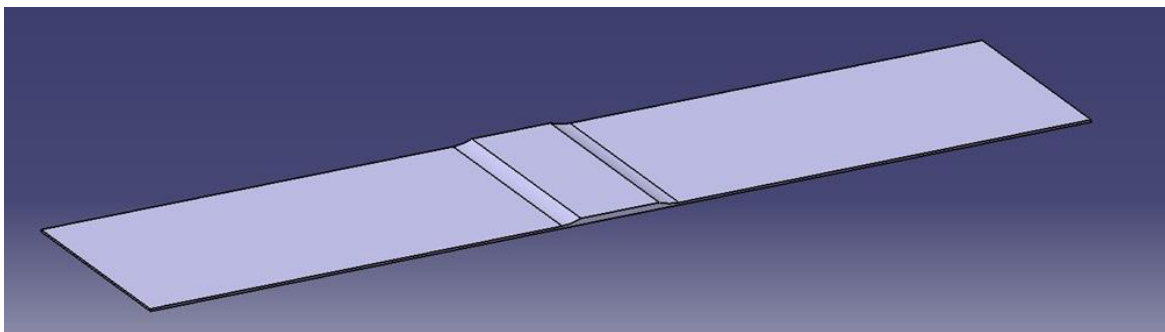
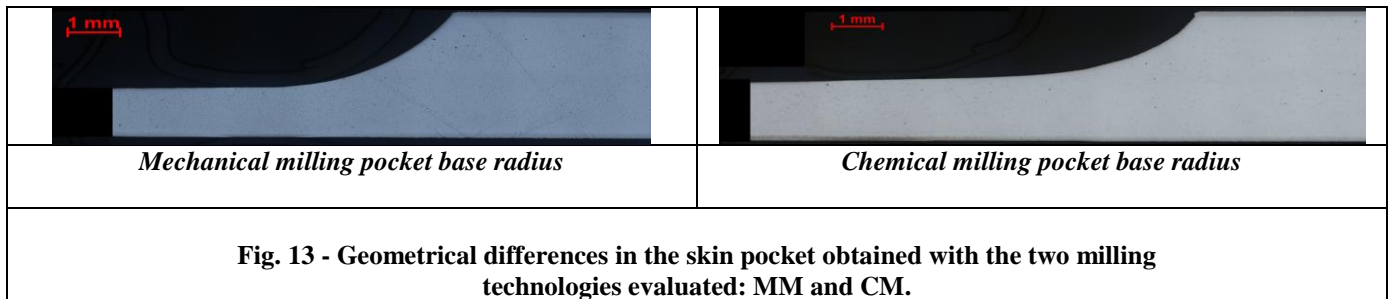


Fig. 14 – Sketch of a specimen geometry for fatigue assessment of the milling technology.

Group	Grain Dir.	Kt	Stress Ratio	Temp.
1	L	1	0.1	RT
2	L	1	-1	RT
3	T	1	-1	RT
3a	T	1	0.1	RT
4	L	1	-1	400°C
5	T	1	-1	400°C
6	L	3	0.1	RT
7	L	3	-1	RT

Table I - Test matrix relevant to the Inconel 718 fatigue program.

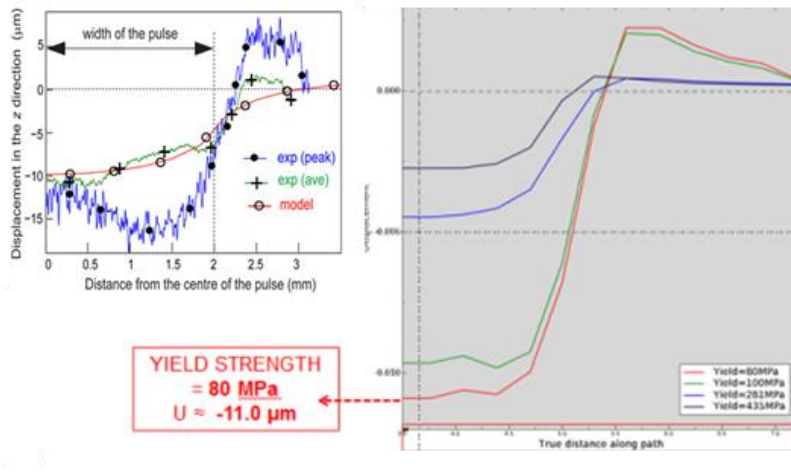


Figure 18 - LSP numerical simulation: comparison between experimental measurement of displacement and numerical analyses with modified Johnson-Cook parameters

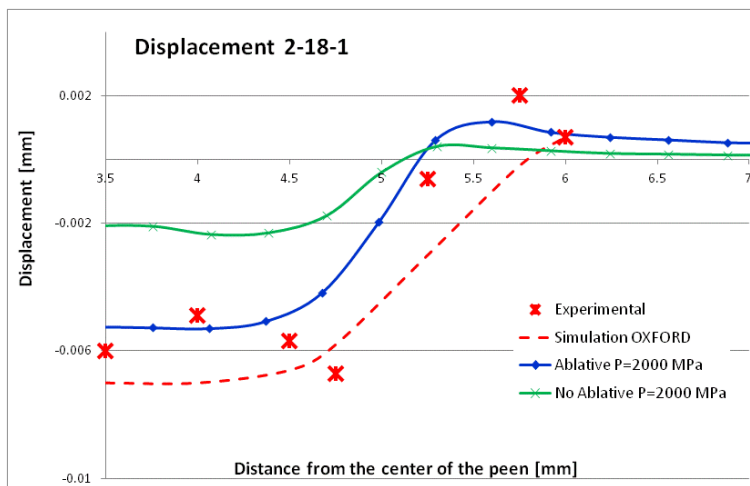


Figure 19 - LSP numerical simulation: numerical – experimental comparison of displacements for 2-18-1 laser configuration.

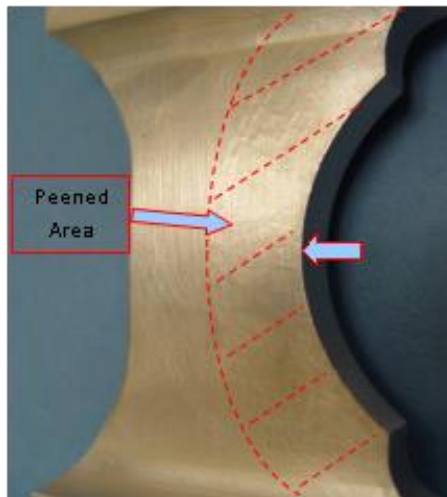


Figure 20 - EADS-IW LSP specimen geometry.

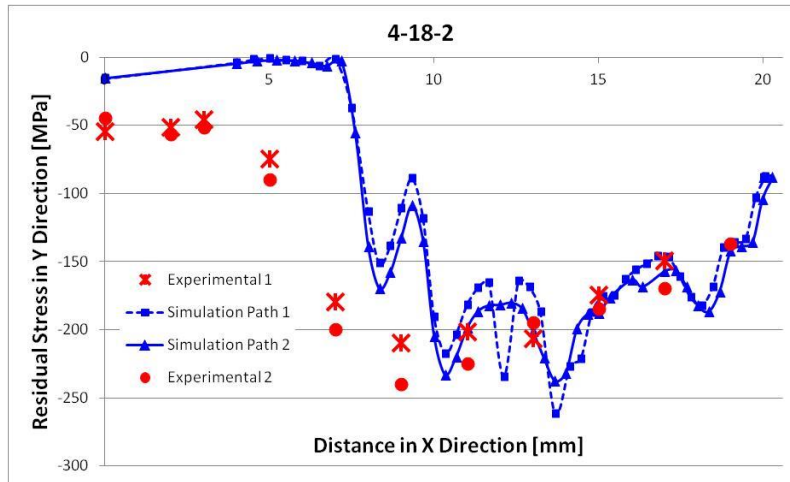


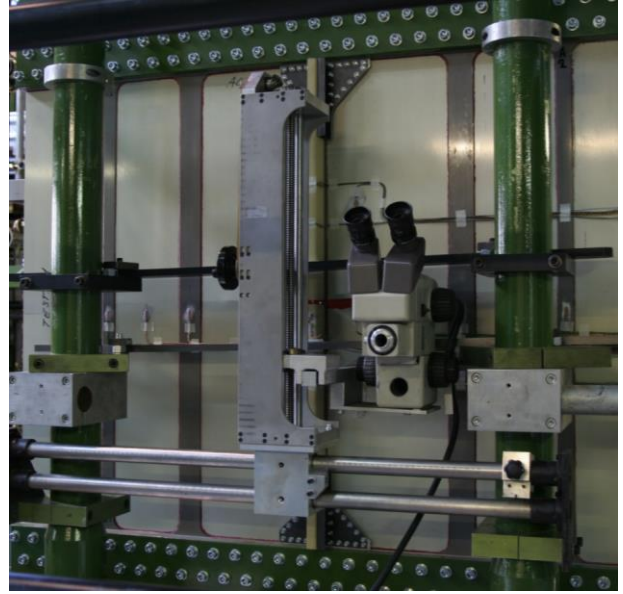
Figure 21 - LSP numerical simulation: numerical – experimental comparison of residual stresses for 4-18-2 laser configuration.



a) General view (skin side)



b) Detail - skin side



c) Detail - pad side

Fig. 22 - Piaggio Aero Industries PIXX damage tolerance development test set-up

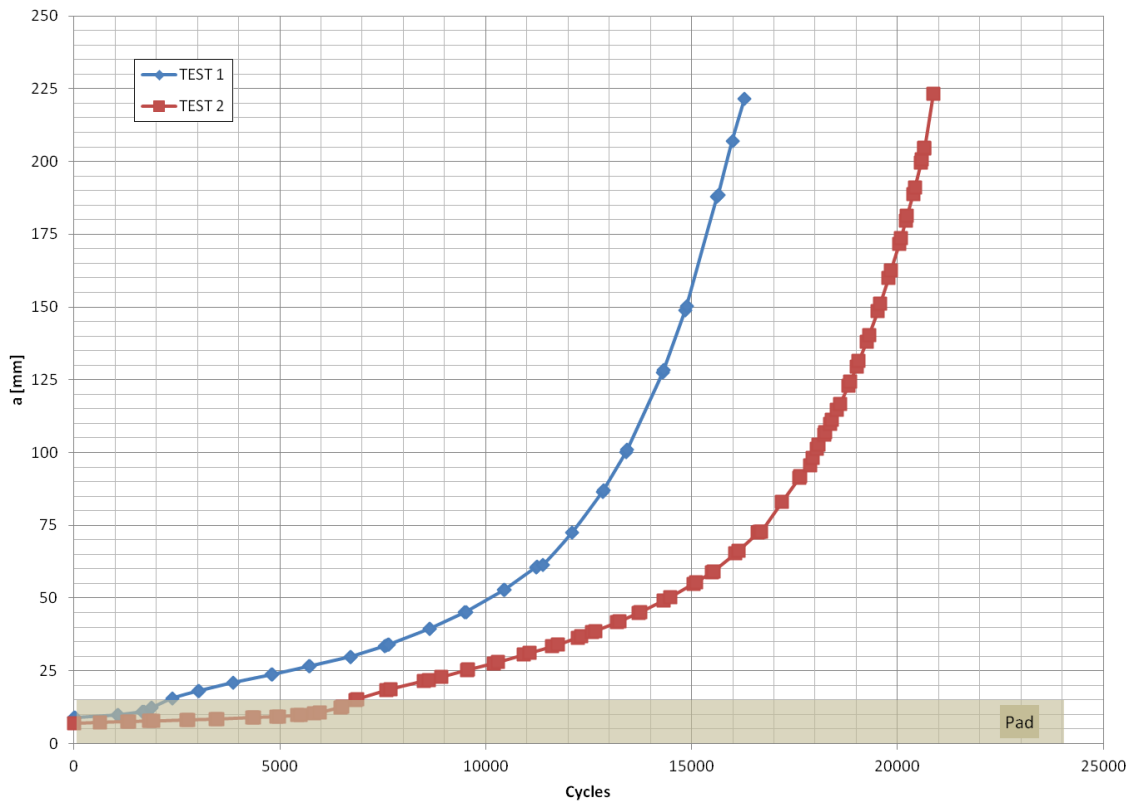


Figure 23 - PIXX damage tolerance development test: summary of a-N results.

TEST 2

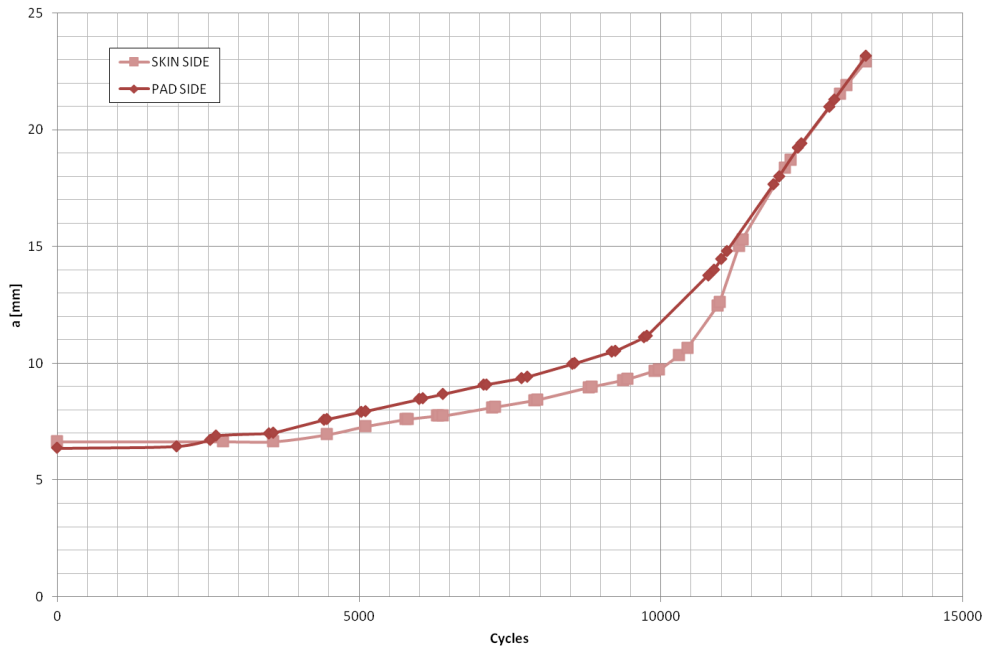


Figure 24 - Detail of the crack growth results: influence of secondary bending.

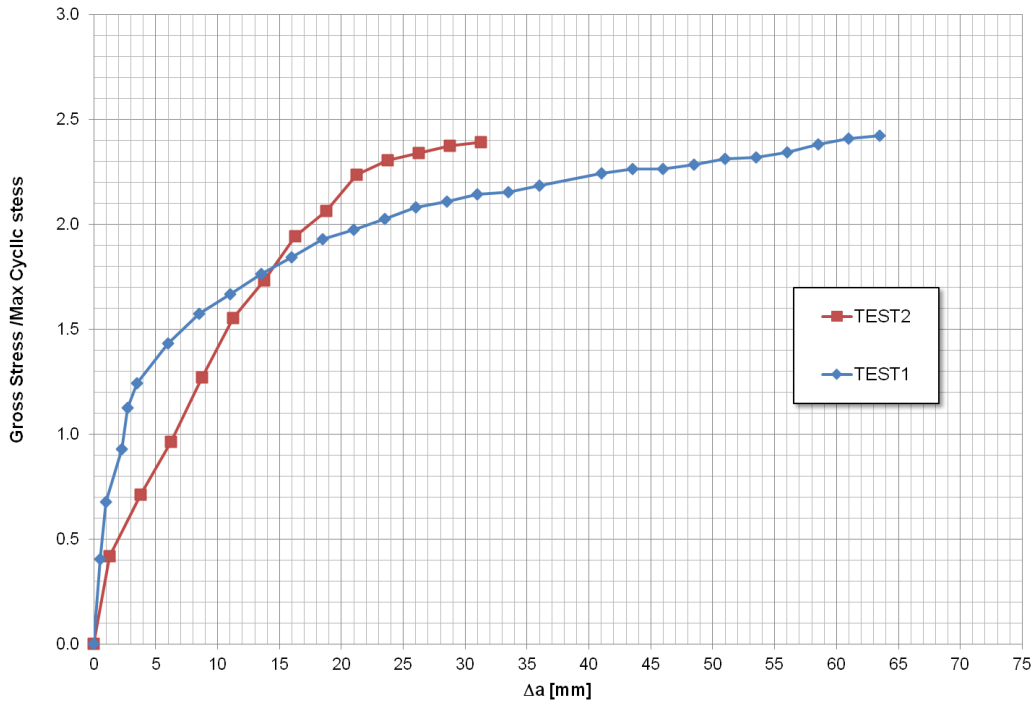


Fig. 25 - PIXX damage tolerance development test: residual static test results, in terms of mean gross stress vs. stable crack growth.

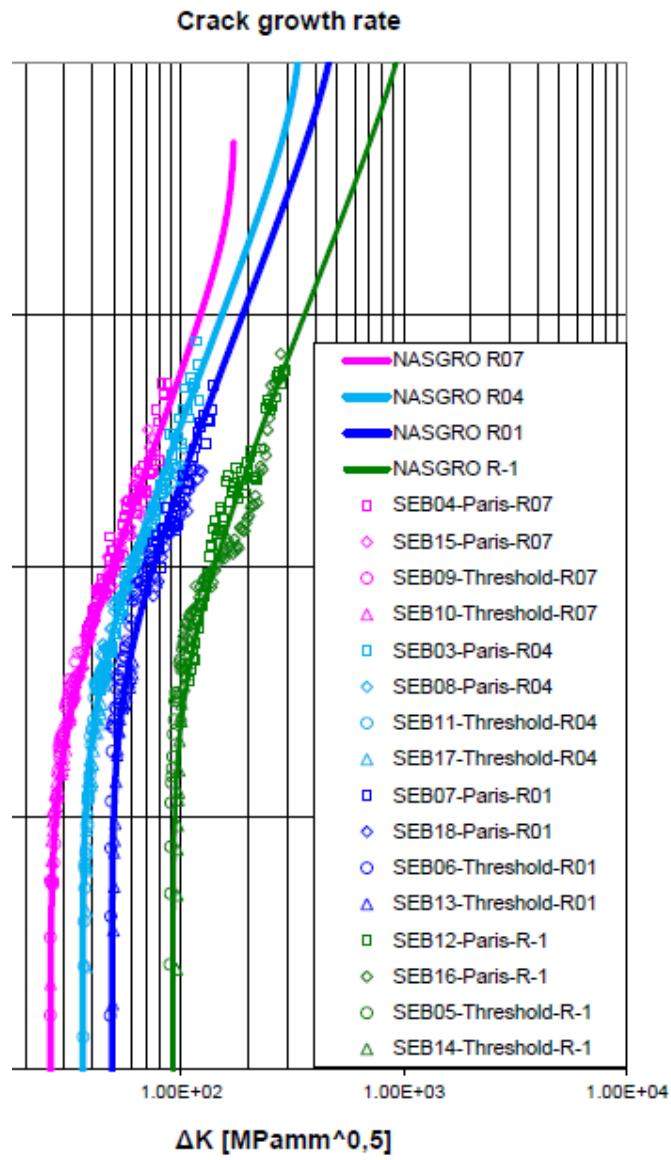


Fig. 26 - Fatigue crack propagation results in Elektron 21 Mg casting alloy.

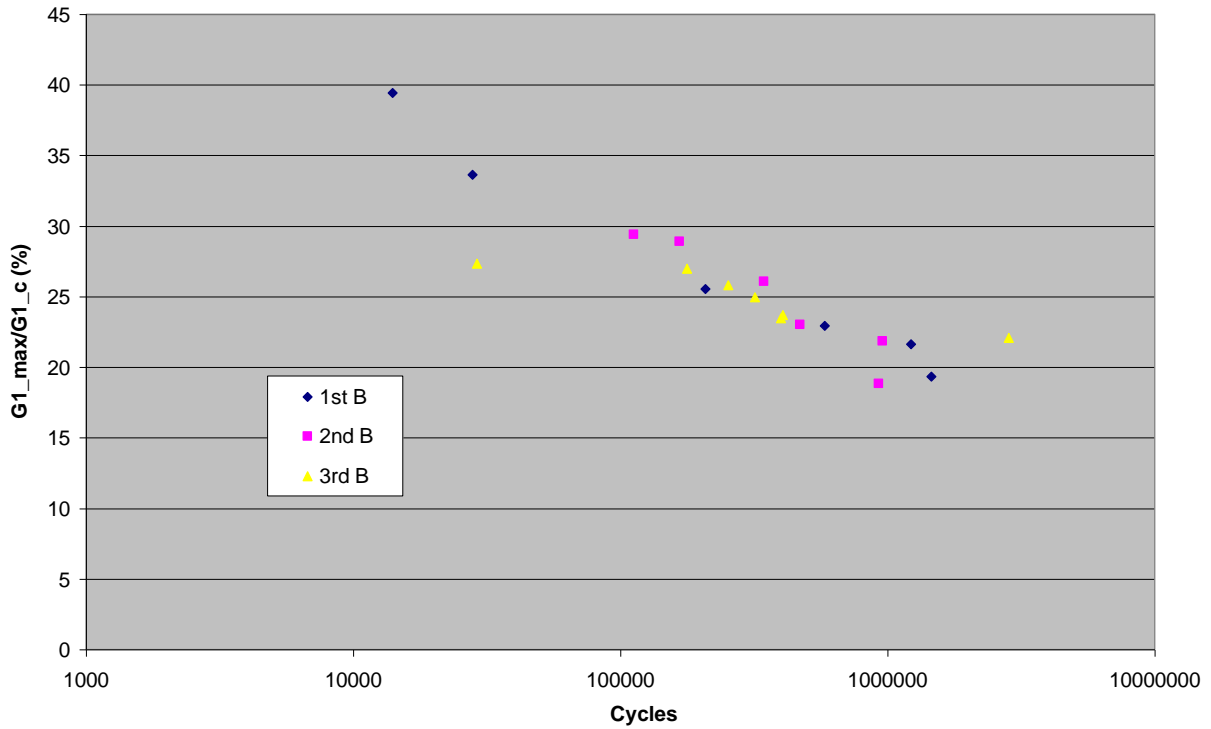


Fig. 27 - Experimental results of fatigue tests for delamination onset in DCB made of S2-5216.

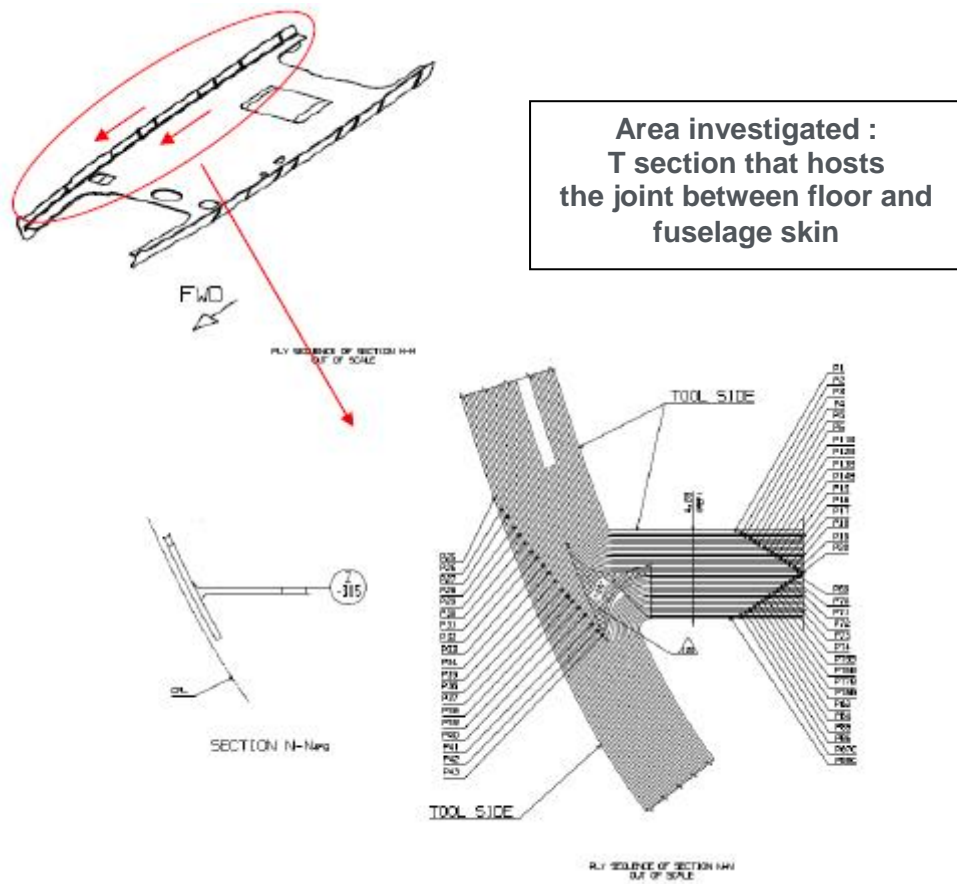


Fig. 28 - M346 CFRP cabin floor to fuselage joint.

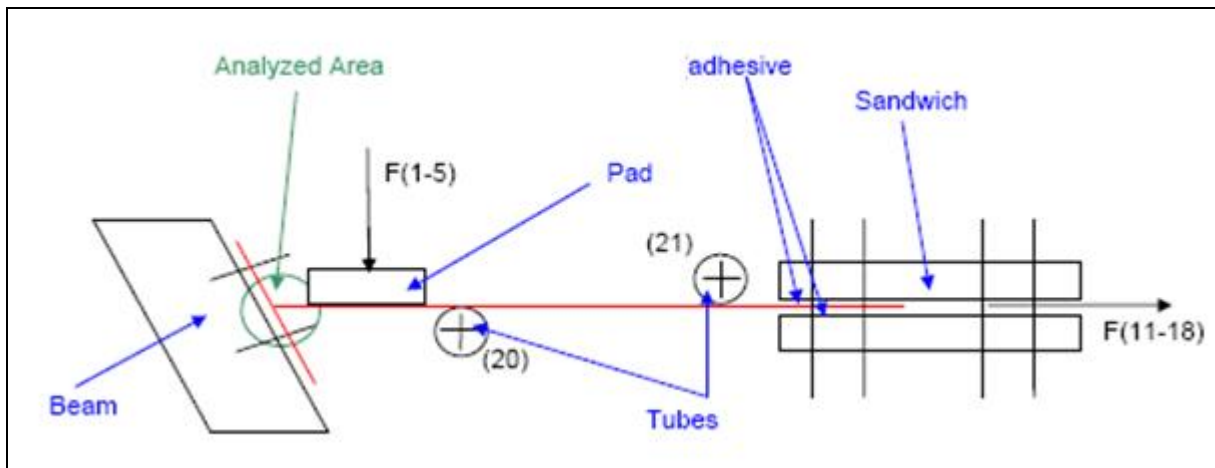


Fig. 29 - Sketch of the set-up for the M346 CFRP cabin floor to fuselage joint fatigue test.

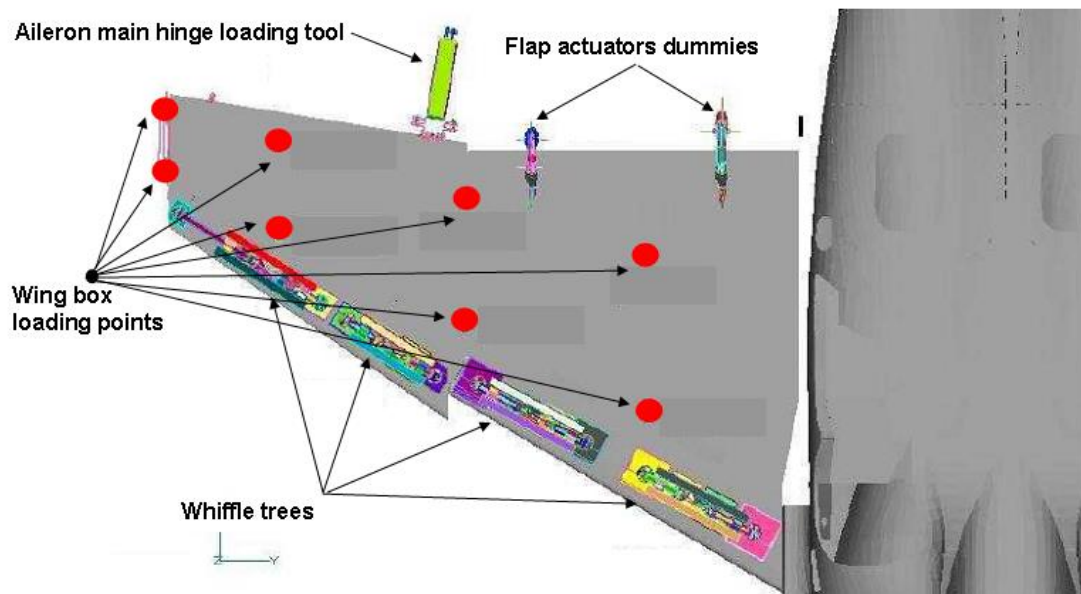


Fig. 30 - Position of load introduction points in the wing of the M346 Full Scale Fatigue Test

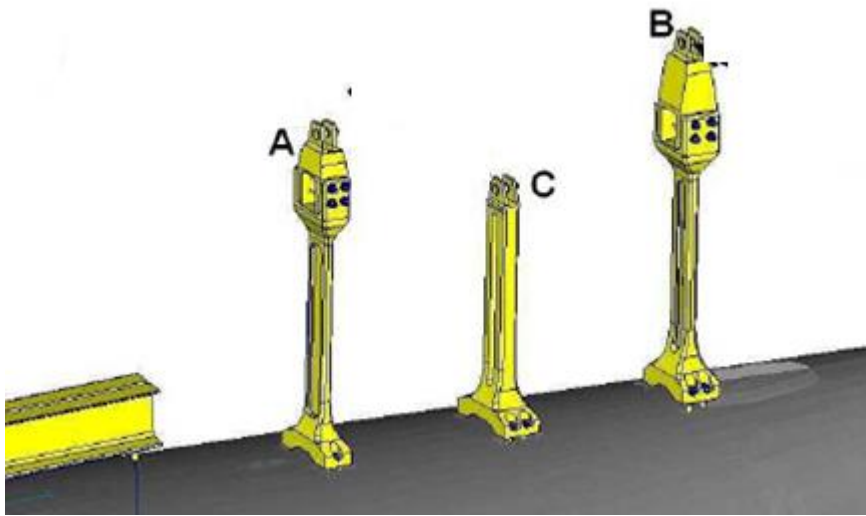


Fig. 31 - Sketch of the M-346 VT dummy and load introduction points.



Fig. 32 - Picture of the M-346 HT fatigue test set-up.

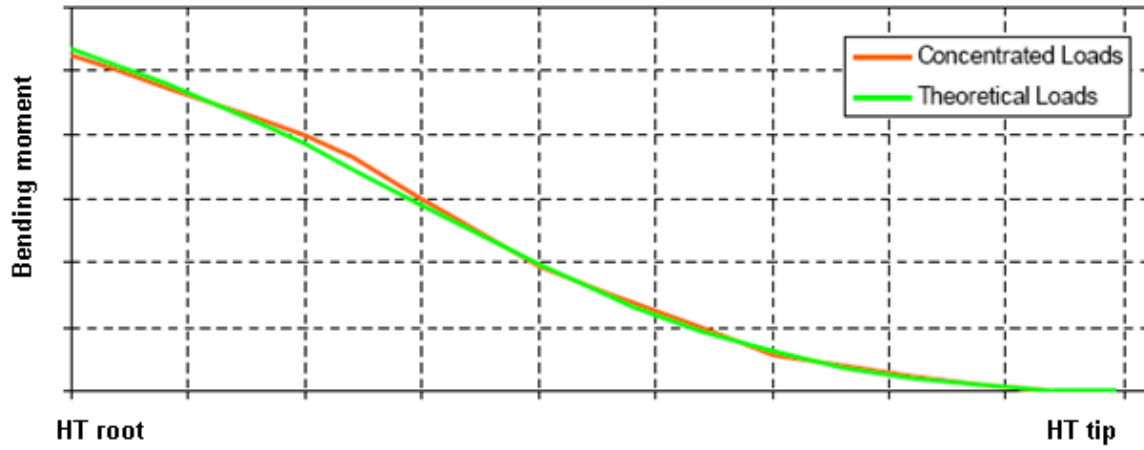


Fig. 33 - Comparison between theoretical bending distribution in the M-346 HT and the one obtained by means of concentrated load introduction.



Fig. 34 - Picture of the M-346 VT fatigue test set-up.

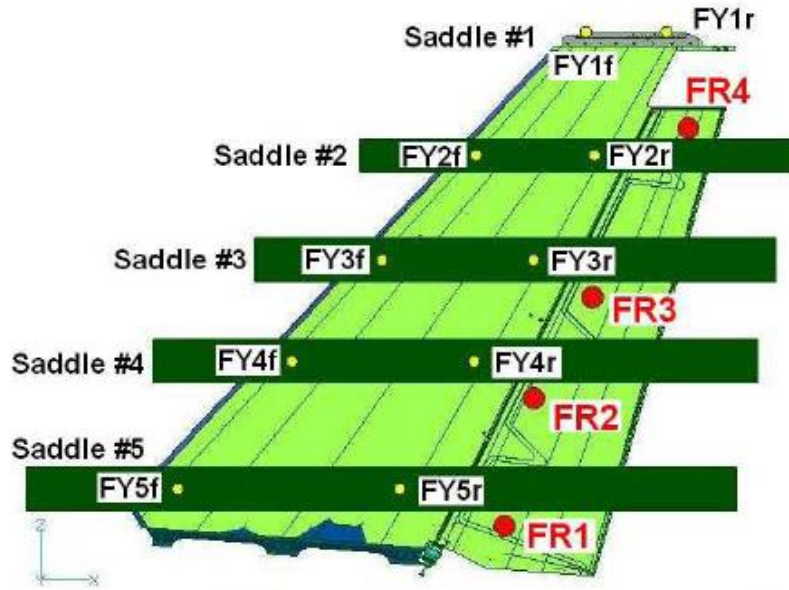


Fig. 35 - Position of the load introduction points in the M-346 HT fatigue test set-up.

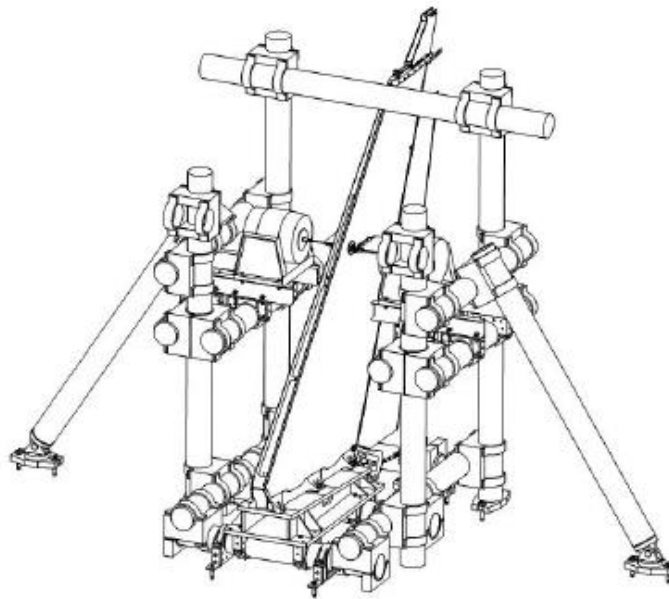


Fig. 36 - Position of the shakers in the M-346 VT fatigue test set-up.

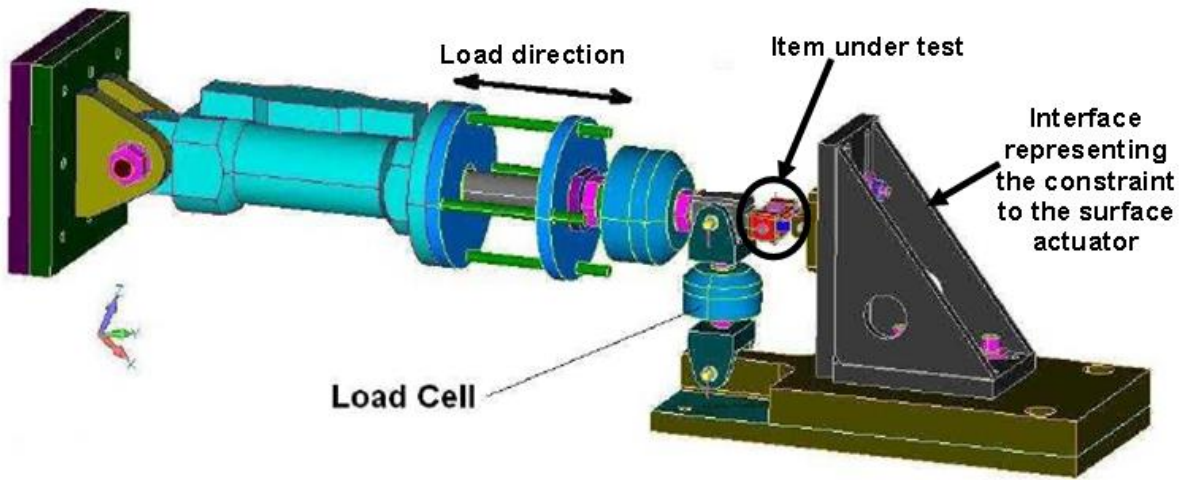


Fig. 37 - M-346 outer droop nose balance durability and damage tolerance test rig set-up.



Fig. 38 - C-Series Bombardier program: example of element and sub-component tests.

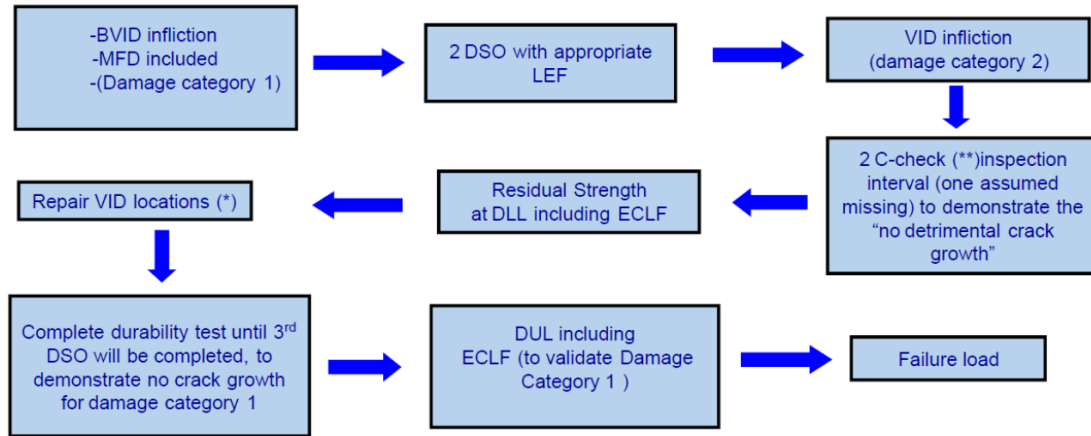


Fig. 39 - Procedure to be followed in the performance of the Bombardier CSeries Full Scale Fatigue Test.